Weak Form of the Stokes-Dirac Structure and Geometric Discretization of Port-Hamiltonian Systems

P Kotyczka, B. Maschke, Laurent Lefèvre

Weak Form of the Stokes-Dirac Structure and Geometric Discretization of Port-Hamiltonian Systems

P. Kotyczka, B. Maschke, L. Lefèvre

May 18, 2017

Abstract

We present the mixed Galerkin discretization of distributed-parameter port-Hamiltonian systems. Due to the inherent definition of (boundary) interconnection ports, this system representation is particularly useful for the modeling of interconnected multi-physics systems and control. At the prototypical example of a system of two conservation laws in arbitrary spatial dimension, we derive the main contributions: (i) A weak formulation of the underlying geometric (Stokes-Dirac) structure, (ii) its geometric approximation by a finite-dimensional Dirac structure using a mixed Galerkin approach and power-preserving maps on the space of discrete power variables and (iii) the approximation of the Hamiltonian to obtain finite-dimensional port-Hamiltonian state space models. The power-preserving maps on the discrete bond space offer design degrees of freedom for the discretization, which is illustrated at the example Whitney finite elements on a 2D simplicial triangulation. The resulting schemes can be considered as trade-offs between centered approximations and upwinding.

Keywords: Open systems of conservation laws, port-Hamiltonian systems, mixed Galerkin methods, geometric discretization, structure-preserving discretization.

1 Introduction

The *port-Hamiltonian* (PH) approach for the modeling, interconnection and control of multi-physics systems underwent an enormous evolution during the past two decades. In this article, we concentrate on distributed-parameter PH systems as initially presented in [60], and refer the reader to the books [23], [35] and [63] for a more general overview on theory and applications. The salient feature of PH systems is their representation in terms of (i) a *linear geometric structure* – a *Stokes-Dirac structure* – that describes the power flows inside the system and over its boundary and (ii) an energy functional (or more generally a potential) from which the constitutive or closure relations are derived, and which determines the nature of the systems. Hence, completely different systems – linear/nonlinear or hyperbolic/parabolic [67] – can share the same interconnection structure. PH systems are by definition *open systems*, they interact with their environment through *boundary ports*. The *in-* and *outputs* in the sense of systems' theory and control are defined via a duality product whose value equals the exchanged power at the port. The appropriate definition of boundary port variables plays a crucial role in showing that a PH system is a well-posed boundary control systems [39]. The reasonable definition of distributed power variables as in- and outputs is discussed in [43].

The simulation and control by numerical methods, of complex (in the sense of their geometry, their nonlinearities, their extent, their couplings) distributed-parameter PH systems, requires a spatial discretization, which shall retain the underlying geometric properties related to *power continuity*. According to the separation of the interconnection structure from the constitutive equations, a *geometric discretization* consists of two steps:

- Finite-dimensional approximation of the underlying Stokes-Dirac structure. The duality between the power variables variables (their duality product has the interpretation of power) must be mapped onto the finite-dimensional approximation. This requires a *mixed* approach with different approximation spaces for each group of dual power variables (called flows and efforts). The subspace of discrete power variables on which (the preserved) power-continuity holds, defines a Dirac structure as a finite-dimensional counterpart of the Stokes-Dirac structure.

- The discretization of the interconnection structure is followed by an appropriate discretization of the Hamiltonian and the closure equations, again taking into account the different nature of the approximation spaces.

A geometric discretization is, hence, a *compatible* discretization as defined in [9]: "*Compatible discretizations transform partial differential equations to discrete algebraic problems that mimic fundamental properties of the continuum equations.*" The *open* character of PH systems requires special attention to the treatment of the boundary port variables, in particular the boundary inputs which are imposed as boundary conditions.

The first approach for a geometric or *structure-preserving* discretization of PH systems [29], application to a diffusive process in [7], is based on the idea of mixed finite elements. The Stokes-Dirac structure is, however, discretized in *strong form* which produces restrictive compatibility conditions. In the 1D pseudo-spectral method [42], the degeneracy of the discrete duality product is rectified by the definition of reduced effort variables, see also the recent paper [64] for the application to plasma dynamics described by a parabolic PDE. The reduction of the discrete effort space is generalized by the power-preserving maps in the present paper. In [**?**], the Stokes-Dirac structure is reformulated, changing the role of state and co-state variable for one conservation law. The discrete power-variables are immediately connected with a non-degenerate duality pairing, at the price of a metric-dependent interconnection structure. The *simplicial* discretization of PH systems based on *discrete exterior calculus* has been introduced in [56], see [38] for the extended definition of boundary inputs and a revised interpretation of the resulting state space models. Recently, the very related discretization on staggered grids has been reported using finite volumes [37] and finite differences [58].

The *weak* or *variational* formulation as the basis for Galerkin numerical approximations, including the different varieties of the finite element method (see [47], to cite only one textbook), has been only rarely used for modeling and discretization of PH systems: In [**?**], one of the two conservation laws is written in weak form. [2] presents the PH model of the reactive 1D Navier-Stokes equations in weak form. In [17], a piezo patch on a flexible beam, with a discontinuous spatial distribution, is included in the PH model and its structure preserving discretization via the weak form.

In this article, we present the geometric discretization of distributed-parameter PH systems based on the *weak* or *variational formulation* of the underlying Stokes-Dirac structure. Doing so, some limitations and restrictions of current approaches for PH systems can be overcome.

- The formulation is valid for systems on spatial domains with arbitrary dimension.
- PH systems with non-canonical system operators (containing e.g. higher order derivatives) can be discretized, as well as systems with dissipation and/or diffusion.
- In terms of finite elements, approximation spaces with higher polynomial degree can be used.
- Due to the *weak imposition* of boundary conditions, the boundary inputs appear *directly* in the weak form of the Stokes-Dirac structure.
- The power-preserving maps for the discrete power variables offer design degrees of freedom for the resulting PH approximate models. These design parameters can be used to adapt the discretization to the physical nature of the system (e.g. accounting for the ratio between convection and diffusion) and to improve the approximation quality.

We consider as the prototypical example of distributed-parameter PH systems, an *open system of two conservation laws in canonical form*, as presented in [60]. We use the language of differential forms, see e.g. [26], which highlights the geometric nature of each variable and allows for a unifying representation independent of the dimension of the spatial domain.

An important reason for expressing the spatial discretization of PH systems based on the weak form is to make the link with modern geometric discretization methods. Bossavit's work in computational electromagnetism, [11], [12] (based on Whitney elements [66]) and Tonti's cell method [57] keep track of the geometric nature of the system variables which allows for a direct interpretation of the discrete variables in terms of *integral* system quantities. This integral point of view is also adopted in *discrete exterior calculus* [22]. *Finite element exterior calculus* [5] gives a theoretical frame to describe functional spaces of differential forms and their compatible approximations, which includes the construction of higher order approximation bases that generalize the famous *Whitney* forms [66], see also [49]. We refer also to the recent article [33] which proposes *conforming* polynomial approximation bases, in which the conservation laws are *exactly* satisfied, and which gives an excellent introduction to the geometric discretization. Impressing examples for the use of geometric discretization methods can be found in weather prediction [19] or the simulation of large-scale fluid flows [20], where the conservation of potential vorticity plays an important role. Another important aspect of using the weak form as basis for structure-preserving discretization is to make the link with well-known numerical methods and to pave the way for a simulation of PH systems with existing numerical tools like FreeFEM++ [31] or GetDP [28].

The paper is structured as follows. In Section 2 we review the definition of distributed-parameter port-Hamiltonian systems. We focus in particular on systems of two conservation laws and the underlying Stokes-Dirac structure. We introduce the Stokes-Dirac structure with boundary ports of different causality as it will be used in the rest of the paper. In Section 3 we define the weak form of this Stokes-Dirac structure and present its mixed Galerkin approximation. This approximation features, due to the different geometric nature of the power variables and their approximation spaces, a *degenerate* power pairing. In Section 4, new discrete power variables (or bond variables), with a *non-degenerate* duality pairing are defined via *power-preserving maps*. The mixed Galerkin approximation, expressed in the new space of discrete bond variables, defines a finite-dimensional Dirac structure, which admits different representations. The input-output representation, together with the finite-dimensional approximation of the Hamiltonian, leads to the desired port-Hamiltonian approximate models in state space form. Section 5 illustrates the method using Whitney finite elements on a 2D simplicial grid. In particular, we highlight the interpretation of the finite-dimensional state and power variables in terms of integral quantities on the grid. Moreover, we show how discretization schemes with different approximation quality are obtained via the parametrization of the power-preserving maps. Section 6 closes the paper with a summary and an outlook to ongoing and future work.

2 Distributed-Parameter Port-Hamiltonian Systems

2.1 Canonical systems of two conservation laws

We consider *canonical* systems of two conservation laws[1] on an open, bounded and connected n-dimensional spatial domain[2] Ω with Lipschitz boundary $\partial\Omega$ in *port-Hamiltonian* form as described in [60]. We use the language of *differential forms*, see e.g. [26]. Initially, we assume all differential forms to be *sufficiently smooth* and denote $\Lambda^k(\Omega)$ the space of smooth differential k-forms on Ω.

The partial differential equations (PDEs) for this canonical class of PH systems are written as[3]

$$\begin{bmatrix} -\partial_t p(z,t) \\ -\partial_t q(z,t) \end{bmatrix} = \underbrace{\begin{bmatrix} 0 & (-1)^r \mathrm{d} \\ \mathrm{d} & 0 \end{bmatrix}}_{\mathcal{J}_{\text{can}}} \begin{bmatrix} \delta_p H(p(z,t), q(z,t)) \\ \delta_q H(p(z,t), q(z,t)) \end{bmatrix}, \tag{1}$$

with $p(z,t) \in \Lambda^p(\Omega)$, $q(z,t) \in \Lambda^q(\Omega)$ the *state variables* subject to initial conditions $p(z,0) = p_0(z)$, $q(z,0) = q_0(z)$. $\mathcal{J}_{\text{can}}$ denotes a *canonical*, matrix-valued and formally skew-symmetric[4] differential operator with $\mathrm{d} : \Lambda^k(\Omega) \to \Lambda^{k+1}(\Omega)$ the *exterior derivative*. Moreover, $r = pq + 1$[5]. The *Hamiltonian* or

[1] Or a system of two conservation laws with canonical interdomain coupling.

[2] We consider $\Omega \subset \mathbb{R}^n$, however, Ω can be, in general, a smooth manifold.

[3] Here, we indicate the dependencies of the variables on the spatial coordinate $z \in \Omega$ and time $t \in [0, \infty)$. Later on, they will be omitted for brevity.

[4] A *formal* differential operator $\mathcal{J}$ is defined *without* boundary conditions (see e.g. [36], Sect. III.3). Formal skew-symmetry is verified by $\langle \mathbf{e}, \mathcal{J}\mathbf{e} \rangle = -\langle \mathcal{J}\mathbf{e}, \mathbf{e} \rangle$ under *zero* boundary conditions, where $\langle \cdot, \cdot \rangle$ is the inner product on the appropriate functional space.

[5] We use the same symbol for the state variables (as differential forms) and their degrees, which should in general not provoke any confusion.

energy functional is given by

$$H(p(z,t),q(z,t)) = \int_\Omega \mathcal{H}(p(z,t),q(z,t),z) \tag{2}$$

with the *Hamiltonian density* $\mathcal{H} : \Lambda^p(\Omega) \times \Lambda^q(\Omega) \times \Omega \to \Lambda^n(\Omega)$. The vector on the right hand side of (1) contains the *co-energy* or *co-state* variables

$$e^p(z,t) := \delta_p H(p(z,t),q(z,t)) \in \Lambda^{n-p}(\Omega), \quad e^q(z,t) := \delta_q H(p(z,t),q(z,t)) \in \Lambda^{n-q}(\Omega), \tag{3}$$

which are – for the considered class of hyperbolic systems – defined as the *variational derivatives* of the Hamiltonian, i.e. differential forms $\delta_p H$ and $\delta_q H$ that satisfy[6]

$$H(p+\delta p, q+\delta q) = \int_\Omega \mathcal{H}(p,q,z) + \int_\Omega \delta_p H \wedge \delta p + \delta_q H \wedge \delta q \;+\; \mathcal{O}(\delta p^2, \delta q^2). \tag{4}$$

We call the equations to define e^p and e^q *constitutive* or *closure* equations. They determine the *nature* of the system (linear or nonlinear; hyperbolic as considered here or parabolic, see [67]). Comparing the degrees of the co-energy differential forms ($n-p$ and $n-q$) with the degrees for the right hand side of (1) to make sense ($q-1$ and $p-1$) yields the relation $p+q = n+1$ between the dimension of Ω and the degrees of the differential forms[7].

The *boundary port variables* are defined as

$$\begin{bmatrix} f^\partial(z,t) \\ e^\partial(z,t) \end{bmatrix} = \begin{bmatrix} 1 & 0 \\ 0 & (-1)^p \end{bmatrix} \begin{bmatrix} \delta_p H(p(z,t),q(z,t)) \\ \delta_q H(p(z,t),q(z,t)) \end{bmatrix}\Bigg|_{\partial\Omega}, \tag{5}$$

where $(\cdot)|_{\partial\Omega}$ represents the *trace* or *the restriction to the boundary* of a differential form. Imposing the port variables $f^\partial(z,t) \in \Lambda^{n-p}(\partial\Omega)$ and/or $e^\partial(z,t) \in \Lambda^{n-q}(\partial\Omega)$ on a subset of $\partial\Omega$ as *control input* (and understanding the port variables on the remaining boundary as *observation* or *output*), makes the system representation (1), (5) a *boundary control system* in the sense of [24].

For 1D linear PH systems with a *generalized* skew-symmetric system operator, [39] gives conditions on the assignment of boundary in- and outputs for the system operator to generate a contraction semigroup. The latter is instrumental to show *well-posedness* of a linear PH system, see [35]. Essentially, *at most half the number of boundary port variables* can be imposed as control inputs for a well-posed PH system in 1D.

Taking $\delta p = \dot{p}$, $\delta q = \dot{q}$ as variations in (4), and omitting the higher order terms, the time derivative of the energy functional (2) reads[8]

$$\dot{H} = \int_\Omega \delta_p H \wedge \dot{p} + \delta_q H \wedge \dot{q} =: \langle \delta_p H | \dot{p} \rangle_\Omega + \langle \delta_q H | \dot{q} \rangle_\Omega, \tag{6}$$

Replacing $\dot{p}$, $\dot{q}$ according to (1), using the integration-by-parts formula for differential forms and the definition (5) of boundary port variables, yields

$$\dot{H} = \int_{\partial\Omega} (-1)^p \; \delta_q H|_{\partial\Omega} \wedge \delta_p H|_{\partial\Omega} =: (-1)^p \langle \delta_q H | \delta_p H \rangle_{\partial\Omega}. \tag{7}$$

Equating the right hand sides of the last two equations gives a (differential) energy balance equation or a *power continuity equation* that relates the internal power flows (i.e. the lossless exchange of energy between the two energy types) *inside* the domain Ω (6) and the power supplied over the system boundary $\partial\Omega$ (7). Due to the energy exchange over the system boundary, we call (1), (5) an *open* system of two conservation laws in canonical port-Hamiltonian form.

[6]The skew-symmetric wedge product $\wedge : \Lambda^k(\Omega) \times \Lambda^l(\Omega) \to \Lambda^{k+l}(\Omega)$ pairs two differential forms, adding their degrees.
[7]See [60] for several examples
[8]For brevity, all arguments are omitted

Notation 1. $\langle\cdot|\cdot\rangle_\Omega : \Lambda^{n-k}(\Omega) \times \Lambda^k(\Omega) \to \mathbb{R}$ is the short notation for the *duality product*

$$\langle\lambda|\mu\rangle_\Omega := \int_\Omega \lambda \wedge \mu \tag{8}$$

between two differential forms on the n-dimensional domain Ω. Accordingly for $\partial\Omega$.

Example 1 (1D transmission line)**.** The simplest example in 1D of a system of two conservation laws is an electric transmission line with $\Omega = [0, L]$, see e.g. [30]. With $p(z) \in \Lambda^1(\Omega)$, the magnetic flux density one-form, $q(z) \in \Lambda^1(\Omega)$, the electric charge density one-form, $l(z)dz, c(z)dz \in \Lambda^1(\Omega)$ the distributed inductance and capacitance per length (note that in this representation, $l(z)$ and $c(z)$ are functions, i.e. zero-forms), the Hamiltonian density one-form is $\mathcal{H}(p,q) = \frac{1}{2}\left(p(z) \wedge *\frac{p(z)}{l(z)} + q(z) \wedge *\frac{q(z)}{c(z)}\right)$. The *Hodge star* operator $* : \Lambda^k(\Omega) \to \Lambda^{n-k}(\Omega)$ renders in the 1D case a one-form a zero-form and vice-versa[9]. The variational derivatives of the Hamiltonian $H = \int_0^L \mathcal{H}$ turn out to be the current and the voltage along the line, $\delta_p H = *\frac{p(z)}{l(z)} = i(z) \in \Lambda^0(\Omega)$, $\delta_q H = *\frac{q(z)}{c(z)} = u(z) \in \Lambda^0(\Omega)$.

Example 2 (2D shallow water equations)**.** The shallow water equations describe the two-dimensional flow of an inviscid fluid with relatively low depth ("shallow") which permits the averaging of the horizontal components of the velocity field and the omission of the vertical velocity component. The two equations that describe the conservation of mass and momentum over an infinitesimal, fixed surface element[10], are (we consider the fluid in a non-rotating system) can be written in vector calculus notation, see e.g. [25],

$$\begin{aligned} \partial_t h + \operatorname{div}(h\mathbf{u}) &= 0 \\ \partial_t(h\mathbf{u}) + \operatorname{div}(h\mathbf{u}\mathbf{u}) + \frac{1}{2}g\nabla h^2 + gh\nabla z_b &= 0. \end{aligned} \tag{10}$$

h denotes the water level over the bottom, z_b is the vertical coordinate that describes the bottom profile, $\mathbf{u} = [u \quad v]^T$ the 2-dimensional velocity field, $h\mathbf{u} = \mathbf{F}$ the discharge vector and g the gravitational acceleration. $\mathbf{u}\cdot\mathbf{u}$ and $\mathbf{u}\mathbf{u}$ denote the scalar and the tensor (dyadic) product of two vectors, respectively. With some rules of tensor calculus[11], and replacing the continuity equation, the momentum equation can be reformulated in terms of $\mathbf{u}$ and one obtains

$$\begin{bmatrix} \partial_t h \\ \partial_t \mathbf{u} + q\mathbf{F}^\perp \end{bmatrix} = \begin{bmatrix} 0 & -\operatorname{div} \\ -\operatorname{grad} & 0 \end{bmatrix} \begin{bmatrix} \frac{1}{2}\mathbf{u}\cdot\mathbf{u} + gh + gz_b \\ h\mathbf{u} \end{bmatrix}, \tag{11}$$

where $q = \frac{1}{h}(\partial_x v - \partial_y u)$ denotes the *potential vorticity*[12], and $\mathbf{F}^\perp = [hv \quad -hu]^T$. The term $q\mathbf{F}^\perp$ represents the acceleration of the fluid due to rotation of the flow. It stems from the rotational part of the transport term in the momentum equation. The total energy (per unit mass) is

$$H = \int_\Omega \frac{1}{2}h\mathbf{u}\cdot\mathbf{u} + \frac{1}{2}gh^2 + ghz_b\, d\mathbf{x}. \tag{12}$$

To rewrite the equations in terms of differential forms (in a covariant formulation), we use the relations, see [1][13]

$$\nabla f = (\mathrm{d}f)^\sharp, \quad \operatorname{div}\mathbf{f} = *\mathrm{d}(*\mathbf{f}^\flat). \tag{13}$$

[9] The *Hodge star* induces an *inner product* on the space of differential forms on a manifold M by

$$(\alpha, \beta) := \int_M \alpha \wedge *\beta = \int_M \beta \wedge *\alpha = (\beta, \alpha), \qquad \alpha, \beta \in \Lambda^k(M). \tag{9}$$

see Section 8.4 of [26] or Section 3.6 of [34]. The inner product is not necessarily the standard L^2 norm, but may be equipped with another metric, see e.g. the energy norm fo linear PH systems [35]. The Hodge star is, hence, *metric* dependent.

[10] Which corresponds to the *Eulerian* representation of the fluid flow.

[11] See appendix A.4 of [8]: $\nabla\cdot(s\mathbf{I}) = \nabla s$, $\nabla\cdot(\mathbf{v}\mathbf{w}) = \mathbf{v}\cdot\nabla\mathbf{w} + \mathbf{w}(\nabla\cdot\mathbf{v})$, $\mathbf{v}\cdot\nabla\mathbf{v} = \frac{1}{2}\nabla(\mathbf{v}\cdot\mathbf{v}) - \mathbf{v}\times(\nabla\times\mathbf{v})$. The last term with cross product and rotation has to be evaluated based on the 3D velocity vector with zero vertical component.

[12] The potential vorticity satisfies the balance equation $\partial_t q + \mathbf{u}\cdot\nabla q = 0$, i.e. it is advected with the fluid flow see e.g. [4]. It plays an important role in the long-time numerical simulation of large scale flow problems, see e.g. [51].

[13] Index raising ($\sharp$) produces a vector field with the same components from a one-form. Index lowering ($\flat$) produces a one-form with identical components from a vector field. Raising and lowering refers to the fact that upper (lower) indices are typically used for the components of vector fields (one-forms).

Taking into account that $**\lambda = (-1)^{k(n-k)}\lambda$ for a k-form λ, we obtain

$$\begin{bmatrix} -\partial_t(*h) \\ -(\partial_t \mathbf{u} + q\mathbf{F}^\perp)^\flat \end{bmatrix} = \begin{bmatrix} 0 & -\mathrm{d} \\ \mathrm{d} & 0 \end{bmatrix} \begin{bmatrix} p_{dyn} \\ -(*\mathbf{F}^\flat) \end{bmatrix}, \tag{14}$$

where $*h \in \Lambda^2(\Omega)$ and $\mathbf{u}^\flat \in \Lambda^1(\Omega)$ are the 2-form and 1-form associated with the water depth and the flow velocity ($p = 2$, $q = 1$). $p_{dyn} = \frac{1}{2}\mathbf{u}\cdot\mathbf{u} + gh + gz_b \in \Lambda^0(\Omega)$ is the hydrodynamic pressure function (0-form) and $*\mathbf{F}^\flat \in \Lambda^1(\Omega)$ is the 1-form associated to the discharge per unit width. Indeed the vector on the right can be expressed in terms of the variational derivatives $p_{dyn} = \delta_{*h}H$ and $-(*\mathbf{F}^\flat) = \delta_{\mathbf{u}^\flat}H$ of the Hamiltonian $H = \int_\Omega \mathcal{H}$ density 2-form[14] $\mathcal{H} = \frac{1}{2}h(\mathbf{u}^\flat \wedge *\mathbf{u}^\flat) + \frac{1}{2}gh*h + g*hz_b$. If the rotational term $q\mathbf{F}^\perp$ can be neglected[15], (14) has the canonical structure (1).

2.2 Stokes-Dirac structures and port-Hamiltonian systems

Power continuity is a property of the *underlying linear geometric structure* that relates the dual power variables of the system, independent of the *closure equations* for the co-state variables. Defining the distributed and boundary *flow* and *effort* differential forms as

$$\begin{bmatrix} f^p \\ f^q \end{bmatrix} := \begin{bmatrix} -\partial_t p \\ -\partial_t q \end{bmatrix}, \qquad \begin{bmatrix} e^p \\ e^q \end{bmatrix} := \begin{bmatrix} \delta_p H \\ \delta_q H \end{bmatrix}, \qquad \begin{bmatrix} f^\partial \\ e^\partial \end{bmatrix} := \begin{bmatrix} \delta_p H \\ (-1)^p \delta_q H \end{bmatrix}\Bigg|_{\partial\Omega}, \tag{15}$$

the *Stokes-Dirac structure* describes a linear subspace of the *bond space*[16] $\mathcal{F} \times \mathcal{E}$,

$$\begin{aligned} \mathcal{F} &= \Lambda^p(\Omega) \times \Lambda^q(\Omega) \times \Lambda^{n-p}(\partial\Omega) \\ \mathcal{E} &= \Lambda^{n-p}(\Omega) \times \Lambda^{n-q}(\Omega) \times \Lambda^{n-q}(\partial\Omega) \end{aligned} \tag{16}$$

of dual power variables where power continuity

$$\underbrace{\langle e^p | f^p \rangle_\Omega + \langle e^q | f^q \rangle_\Omega}_{\substack{\text{power extracted from} \\ \text{distributed storage}}} \quad + \quad \underbrace{\langle e^\partial | f^\partial \rangle_{\partial\Omega}}_{\substack{\text{power supplied} \\ \text{over the boundary}}} \quad = \quad 0 \tag{17}$$

holds. The Stokes-Dirac structure extends the notion of the finite-dimensional *Dirac structure* to infinite-dimensional systems. The latter can be considered "*the geometrical notion formalizing general power-conserving interconnections*" [60]:

Definition 1 ([60], Def. 2.1)**.** Given the finite-dimensional linear spaces $\mathcal{F}_{\text{fin}}$ and $\mathcal{E}_{\text{fin}}$ over $\mathbb{R}$[17] and a duality pairing $\langle\cdot|\cdot\rangle : \mathcal{F}_{\text{fin}} \times \mathcal{E}_{\text{fin}} \to \mathbb{R}$. Define the symmetric bilinear form

$$\langle\langle(\mathbf{f}_1, \mathbf{e}_1), (\mathbf{f}_2, \mathbf{e}_2)\rangle\rangle := \langle \mathbf{e}_1 | \mathbf{f}_2 \rangle + \langle \mathbf{e}_2 | \mathbf{f}_1 \rangle, \qquad (\mathbf{f}_i, \mathbf{e}_i) \in \mathcal{F} \times \mathcal{E},\ i = 1, 2. \tag{18}$$

A *Dirac structure* is a linear subspace $D_{\text{fin}} \subset \mathcal{F}_{\text{fin}} \times \mathcal{E}_{\text{fin}}$ such that $D_{\text{fin}}^\perp = D_{\text{fin}}$, where $\perp$ denotes the orthogonal complement with respect to the bilinear form $\langle\langle\cdot,\cdot\rangle\rangle$.

From the requirement that each element of a Dirac structure D_{fin} belongs to its orthogonal complement $D_{\text{fin}}^\perp$ (and vice versa), it follows that for all $(\mathbf{f}, \mathbf{e}) \in D_{\text{fin}}$

$$\langle\langle(\mathbf{f}, \mathbf{e}), (\mathbf{f}, \mathbf{e})\rangle\rangle = 2\langle \mathbf{e} | \mathbf{f} \rangle = 0, \tag{19}$$

which is a (finite-dimensional) power-continuity relation as (17). For more details and different representations of Dirac structures (in the PH context) refer to [59], [60].

[14] In 2D we have $*dx = dy$, $*dy = -dx$.

[15] If not, (14) still represents a PH system, as the rotational term does not contribute to the energy balance. It can be associated to a canonical Stokes-Dirac structure, with a different definition of the *dynamic* equation for the 1-form $\mathbf{u}^\flat$.

[16] As a reference to bond graph modeling of dynamical systems [45], see also [23], Chapter 1)

[17] or another field

For the infinite-dimensional *Stokes-Dirac* structure, we consider the duality pairing over differential forms as defined in (8) and the symmetric bilinear form

$$\langle\langle (f_1^p, f_1^q, f_1^\partial, e_1^p, e_1^q, e_1^\partial), (f_2^p, f_2^q, f_2^\partial, e_2^p, e_2^q, e_2^\partial) \rangle\rangle := \\ \langle e_1^p | f_2^p \rangle_\Omega + \langle e_1^q | f_2^q \rangle_\Omega + \langle e_1^\partial | f_2^\partial \rangle_{\partial\Omega} + \langle e_2^p | f_1^p \rangle_\Omega + \langle e_2^q | f_1^q \rangle_\Omega + \langle e_2^\partial | f_1^\partial \rangle_{\partial\Omega} \quad (20)$$

with $(i = 1, 2)$

$$\begin{aligned} f_i^p &\in \Lambda^p(\Omega), & f_i^q &\in \Lambda^q(\Omega), & f_i^\partial &\in \Lambda^{n-p}(\Omega) \\ e_i^p &\in \Lambda^{n-p}(\Omega), & e_i^q &\in \Lambda^{n-q}(\Omega), & e_i^\partial &\in \Lambda^{n-q}(\Omega). \end{aligned} \quad (21)$$

Theorem 1. *([60], Thm. 2.1) The linear subspace of $\mathcal{F} \times \mathcal{E}$, see* (16)*, given by*

$$D = \{(f^p, f^q, f^\partial, e^p, e^q, e^\partial) \in \mathcal{F} \times \mathcal{E} \mid \\ \begin{bmatrix} f^p \\ f^q \end{bmatrix} = \begin{bmatrix} 0 & (-1)^r \mathrm{d} \\ \mathrm{d} & 0 \end{bmatrix} \begin{bmatrix} e^p \\ e^q \end{bmatrix}, \begin{bmatrix} f^\partial \\ e^\partial \end{bmatrix} = \begin{bmatrix} 1 & 0 \\ 0 & (-1)^p \end{bmatrix} \begin{bmatrix} e^p|_{\partial\Omega} \\ e^q|_{\partial\Omega} \end{bmatrix} \}. \quad (22)$$

with $r = pq + 1$ and $|_{\partial\Omega}$ the restriction to the boundary $\partial\Omega$ is a Dirac structure, i.e. $D = D^\perp$ holds with respect to the bilinear mapping defined in (20)*.*

As the application of Stokes' theorem instrumental in showing that the above subspace is a Dirac structure, the so-defined geometric structure is called a *Stokes-Dirac* structure. In order to represent the situation of boundary inputs with different causality in a formally consistent way, we introduce the Stokes-Dirac structure with an alternative designation of boundary port variables.

Corollary 1. *The linear subspace*

$$\hat{D} = \{(f^p, f^q, \hat{e}^\partial, e^p, e^q, \hat{f}^\partial) \in \hat{\mathcal{F}} \times \hat{\mathcal{E}} \mid \\ \begin{bmatrix} f^p \\ f^q \end{bmatrix} = \begin{bmatrix} 0 & (-1)^r \mathrm{d} \\ \mathrm{d} & 0 \end{bmatrix} \begin{bmatrix} e^p \\ e^q \end{bmatrix}, \begin{bmatrix} \hat{e}^\partial \\ \hat{f}^\partial \end{bmatrix} = \begin{bmatrix} 1 & 0 \\ 0 & (-1)^p \end{bmatrix} \begin{bmatrix} e^p|_{\partial\Omega} \\ e^q|_{\partial\Omega} \end{bmatrix} \} \quad (23)$$

with

$$\begin{aligned} \hat{\mathcal{F}} &= \Lambda^p(\Omega) \times \Lambda^q(\Omega) \times \Lambda^{n-q}(\partial\Omega) \\ \hat{\mathcal{E}} &= \Lambda^{n-p}(\Omega) \times \Lambda^{n-q}(\Omega) \times \Lambda^{n-p}(\partial\Omega) \end{aligned} \quad (24)$$

is a Dirac structure.

We can understand the representation of the Hamiltonian systems with canonical interdomain coupling (1), (5) as the composition of an underlying geometric *interconnection* for the pairs of *port variables* (f^p, e^p), (f^q, e^q), (f^∂, e^∂) with *dynamic* and *closure* equations (15).

Definition 2. ([60], Def. 2.2, Prop. 2.1) The distributed-parameter system on a closed and bounded n-dimensional manifold Ω with boundary $\partial\Omega$, defined by (1), (5) with Hamiltonian $H(p, q) = \int_\Omega \mathcal{H}(p, q, z)$ and Hamiltonian density $\mathcal{H} : \Lambda^p(\Omega) \times \Lambda^q(\Omega) \times \Omega \to \Lambda^n(\Omega)$, with $p + q = n + 1$ and $r = pq + 1$ is a *port-Hamiltonian system.* It represents an *open* system of two conservation laws and satisfies the energy balance equation (7).

Remark 1. Note that a Stokes-Dirac structure does not lead necessarily to the PH representation of a *hyperbolic system of conservation laws* as in the two examples above. With the corresponding definition of flow and effort variables and closure equations, *parabolic* phenomena based on irreversible conservation laws of thermodynamics (heat conduction) can be modeled based on the *same* canonical Stokes-Dirac structure. See the 3D heat conduction example in [23] (Section 4.2.2, p. 233) or the relation [67].

2.3 Boundary ports

The choice of boundary port variables to define a Stokes-Dirac structure (an infinite-dimensional PH system) is not unique, see [39] for the 1D case. On parts of the boundary, e^q may define the control input, while, vice versa, this role is assigned to e^p on the rest. The only constraint on the definition of pairs of boundary port variables is that their entirety reflects the power flow over the boundary as indicated in (7).

In order to represent a larger class of boundary control problems for systems of two conservation laws, the following proposition generalizes the definition of the Stokes-Dirac structure to *multiple* pairs of in- and outputs on $\partial\Omega$ with *different causality.*

Proposition 1. *Given the n-dimensional open and connected domain Ω with Lipschitz boundary $\partial\Omega$. Consider $\partial\Omega$ completely covered by subsets $\Gamma_i \subset \partial\Omega$, $i = 1, \dots, n_\Gamma$, and $\hat{\Gamma}_j \subset \partial\Omega$, $j = 1, \dots, \hat{n}_\Gamma$ with orientation according to $\partial\Omega$. Let $\bigcup_{i=1}^{n_\Gamma} \Gamma_i \cup \bigcup_{j=1}^{\hat{n}_\Gamma} \hat{\Gamma}_j = \partial\Omega$ and the intersections $\Gamma_i \cap \hat{\Gamma}_j$ are either empty or have dimension $n-1$. Define the boundary flow and effort forms*

$$\begin{aligned} f_i^\Gamma &= e^p|_{\Gamma_i}, & \hat{f}_j^\Gamma &= (-1)^p\, e^q|_{\hat{\Gamma}_j}, \\ e_i^\Gamma &= (-1)^p\, e^q|_{\Gamma_i}, & \hat{e}_j^\Gamma &= e^p|_{\hat{\Gamma}_j}, \end{aligned} \tag{25}$$

such that the bond space $\mathcal{F} \times \mathcal{E}$ is composed of[18]

$$\begin{aligned} \mathcal{F} &= \Lambda_\Omega^p \times \Lambda_\Omega^q \times \Lambda_{\Gamma_1}^{n-p} \times \dots \times \Lambda_{\Gamma_{n_\Gamma}}^{n-p} \times \Lambda_{\hat{\Gamma}_1}^{n-q} \times \dots \times \Lambda_{\hat{\Gamma}_{\hat{n}_\Gamma}}^{n-q} \\ \mathcal{E} &= \Lambda_\Omega^{n-p} \times \Lambda_\Omega^{n-q} \times \Lambda_{\Gamma_1}^{n-q} \times \dots \times \Lambda_{\Gamma_{n_\Gamma}}^{n-q} \times \Lambda_{\hat{\Gamma}_1}^{n-p} \times \dots \times \Lambda_{\hat{\Gamma}_{\hat{n}_\Gamma}}^{n-p}. \end{aligned} \tag{26}$$

The subspace $D \subset \mathcal{F} \times \mathcal{E}$, on which

$$\begin{bmatrix} f^p \\ f^q \end{bmatrix} = \begin{bmatrix} 0 & (-1)^r \mathrm{d} \\ \mathrm{d} & 0 \end{bmatrix} \begin{bmatrix} e^p \\ e^q \end{bmatrix} \tag{27}$$

holds and the boundary ports are defined as in (25)*, is a Dirac structure.*

Proof. First observe that with the choice of boundary ports, and by construction of the subsets Γ_i and $\hat{\Gamma}_j$, the boundary power flow can be expressed as

$$\sum_{i=1}^{n_\Gamma} \langle e_i^\Gamma | f_i^\Gamma \rangle_{\Gamma_i} + \sum_{j=1}^{\hat{n}_\Gamma} \langle \hat{f}_j^\Gamma | \hat{e}_j^\Gamma \rangle_{\hat{\Gamma}_j} = (-1)^p \langle e^q | e^p \rangle_{\partial\Omega}. \tag{28}$$

The proof that the above subspace is a Dirac structure, consists of appropriately decomposing Ω and exploiting the *compositionality* property, see Remark 2.2 of [60], of the Stokes-Dirac structure on each subset.

1. Decompose Ω in a set of n-dimensional submanifolds Ω_k and $\hat{\Omega}_l$, with the same orientation as $\partial\Omega$ on $\partial\Omega_k \cap \partial\Omega$ and $\partial\hat{\Omega}_l \cap \partial\Omega$. On each subset, a Stokes-Dirac structure is defined, in an alternating manner, according to Theorem 1 and Corollary 1, respectively. Then $\bigcup_k \partial\Omega_k \cap \partial\Omega = \bigcup_i \Gamma_i$, $\bigcup_l \partial\hat{\Omega}_l \cap \partial\Omega = \bigcup_j \hat{\Gamma}_j$ and $\Gamma_i \cap \partial\Omega_{kl} = \emptyset$, $\hat{\Gamma}_j \cap \partial\hat{\Omega}_{lk} = \emptyset$ for all i, j, k, l. $\partial\Omega_{kl} = -\partial\hat{\Omega}_{lk}$ denotes the common part of the boundary of Ω_k and $\hat{\Omega}_l$, respectively, where the minus sign underscores the inverse orientation by construction. For an illustration of the case $n = 2$, see Fig. 1.

2. Define on each common boundary $\partial\Omega_{kl} = -\partial\hat{\Omega}_{lk}$ the interconnection conditions $f_k^{kl} = e^p|_{\partial\Omega_{kl}} = \hat{e}_l^{lk}$ and $e_k^{kl} = (-1)^p e^q|_{\partial\Omega_{kl}} = \hat{f}_l^{lk}$. Then, the terms $\langle e_k^{kl} | f_k^{kl} \rangle_{\partial\Omega_{kl}}$ and $\langle \hat{f}_l^{lk} | \hat{e}_l^{lk} \rangle_{\partial\hat{\Omega}_{lk}}$ in the overall power continuity equation cancel each other out due to the reverse integration direction. The interconnection is hence power-preserving, and the composition of the separate Stokes-Dirac structures is a Stokes-Dirac structure due to their *compositionality* property. □

Remark 2. In the above proposition, boundary efforts and flows are defined as pure restrictions of either of the distributed efforts to the corresponding subsets Γ_i, $\hat{\Gamma}_j$ of the boundary. It is, however, also possible to define *mixed* boundary variables (e.g. *scattering* variables), as long as the boundary power continuity equation (28) holds. Such a more general parametrization of boundary in- and outputs is presented in [39] for linear 1D PH systems with general skew-symmetric interconnection operators. In- and outputs are characterized such that the resulting system is a boundary control system which is associated to a contraction semigroup.

[18] For brevity, the domain of the differential forms is written as an index, $\Lambda_\Omega^p = \Lambda^p(\Omega)$.

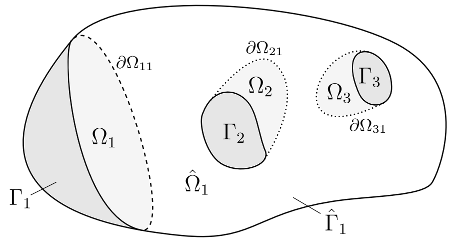

Figure 1: Sketch of a 3-dimensional domain Ω with subdomains Ω_1, Ω_2, Ω_3 and $\hat{\Omega}_1$ and a subdivision of the boundary into $\Gamma_1, \Gamma_2, \Gamma_3$ and $\hat{\Gamma}_1$

Convention 1. In terms of control, we consider the boundary efforts e_i^Γ, $i = 1, \dots n_\Gamma$ and $\hat{e}_j^\Gamma$, $j = 1, \dots, \hat{n}_\Gamma$ as *boundary input* variables, while the boundary flows f_i^Γ, $\hat{f}_j^\Gamma$ are the (power conjugated) *boundary outputs.*

Remark 3. So far, we considered (sufficiently) *smooth* differential forms. Indeed, the (strong) formulation of the Stokes-Dirac structure in Prop. 1 requires that the effort forms are at least continuously differentiable on the closed domain $\overline{\Omega} = \Omega \cup \partial\Omega$, which yields continuous flow differential forms:

$$\begin{aligned} f^p &\in C^0\Lambda^p(\overline{\Omega}), & e^p &\in C^1\Lambda^{n-p}(\overline{\Omega}), \\ f^q &\in C^0\Lambda^q(\overline{\Omega}), & e^q &\in C^1\Lambda^{n-q}(\overline{\Omega}). \end{aligned} \tag{29}$$

The efforts being continuously differentiable on $\overline{\Omega}$, this holds also for their restriction to the boundary $\partial\Omega \subset \overline{\Omega}$:

$$e_i^\Gamma, \hat{f}_j^\Gamma \in C^1\Lambda^{n-q}(\partial\Omega), \quad \hat{e}_j^\Gamma, f_i^\Gamma \in C^1\Lambda^{n-p}(\partial\Omega), \quad i=1,\dots,n_\Gamma,\ j=1,\dots,\hat{n}_\Gamma. \tag{30}$$

Note that with these functional spaces, the duality products (power density integrals) in (17) and (28) are well-defined and finite.

2.4 Further classes of distributed parameter PH systems

In this chapter, we concentrate on *canonical* systems of two conservation laws in *arbitrary* spatial dimension. Beyond this basic class of PH systems (which however covers different linear and nonlinear physical phenomena), there exists a growing number of PH models for different physical phenomena, see e.g. [65] for the modeling of the plasma in a fusion reactor, [3] for the reactive Navier-Stokes flow or [48] for irreversible thermodynamic systems to mention only a few interesting examples. In [46], a PH formulation of the compressible Euler equations in terms of density, weighted vorticity and dilatation is presented.

For the class of linear 1D PH systems represented by general higher order skew-symmetric system operators, the parametrization of in- and outputs to define a boundary control system with a system operator that generates a (contractive or unitary) $\mathcal{C}_0$ semigroup is presented in [39]. The PH representation is not unique. An important approach for mechanical systems is based on a jet bundle formulation [54], see also [53] where the PH formulation of the Mindlin plate based on the jet bundle approach and the Stokes Dirac structure are compared. In [52], different PH representations (symplectic and polysymplectic, both based on jet bundles; Stokes-Dirac structure) which yield different definitions of state variables and Hamiltonian densities, are compared at the illustrative example of the Timoshenko beam.

3 Galerkin approximation of the Stokes-Dirac structure

In this section, we study the *Galerkin approximation* of the Stokes-Dirac structure defined in Prop. 1. To this end, we introduce the *weak form* of the Stokes-Dirac structure and use a *mixed Galerkin* approach to approximate the differential forms according to their geometric nature.

3.1 Weak form of the Stokes-Dirac structure

The first motivation to study the approximation of distributed-parameter PH systems based on their *weak* form is the fact that most of the common numerical methods in engineering, including commercial tools, are based on a Galerkin-type finite-dimensional approximation of the variational problem associated to the PDE. Assuming this perspective is even more natural for system classes, where the PDEs are derived from *variational principles*, as it is the case in structural mechanics[19], see e.g. [50].

Also in the context of existing works on linear port-Hamiltonian distributed-parameter systems in one spatial dimension, this perspective is natural. The statements on well-posedness and stability based on the theory of C_0 semigroups rely on the *mild* solution of the abstract (operator) differential equation. These solutions, however, corresponds to the weak solutions, as known from the theory of PDEs, see [35], page 127: *"In fact, the concept of a mild solution is the same as the concept of a weak solution used in the study of partial differential equations."*

A third point which motivates to discretize port-Hamiltonian distributed-parameter systems based on their weak form, is the close relation of *discrete exterior calculus* (i.e. the mathematical formalism for integral modeling of conservation laws), which has been used in [55] for PH systems: "*Note that the process of integration to suppress discontinuity is, in spirit, equivalent to the idea of weak form used in the Finite Element method.*" [22][20]

Finally, also in the work of Bossavit on the mixed geometric discretization for computational electromagnetism [11], [12], the quality of a *weak* formulation is addressed "*How weak is the weak solution in finite element methods*" [13].

In the following, we will lift the *smoothness* assumption of the differential forms and specify *concrete functional spaces* with conditions on their (weak) differentiability. This is necessary to choose *appropriate basis forms* for the finite-dimensional approximation of the Stokes-Dirac structure. For a quick overview on the necessary notions from functional analysis, we refer to Appendix **??**.

The *weak form* of the Stokes-Dirac structure of Prop. 1 is obtained by a *duality pairing* (which involves exterior multiplication and integration) on Ω with *test forms* of appropriate degree which do *not* vanish on the boundary[21]. The latter allows for a *weak* imposition of the input boundary conditions e_i^Γ, $i = 1, \ldots, n_\Gamma$ and $\hat{e}_j^\Gamma$, $j = 1, \ldots, \hat{n}_\Gamma$.

Definition 3. The weak form of the Stokes-Dirac structure of Prop. 1 is given by the subspace $D \subset \mathcal{F} \times \mathcal{E}$ with[22]

$$
\begin{aligned}
\mathcal{F} &= L^2\Lambda^p_\Omega \times L^2\Lambda^q_\Omega \times L^2\Lambda^{n-p}_{\Gamma_1} \times \cdots \times L^2\Lambda^{n-p}_{\Gamma_{n_\Gamma}} \times L^2\Lambda^{n-q}_{\hat{\Gamma}_1} \times \cdots \times L^2\Lambda^{n-q}_{\hat{\Gamma}_{\hat{n}_\Gamma}} \\
\mathcal{E} &= H^1\Lambda^{n-p}_\Omega \times H^1\Lambda^{n-q}_\Omega \times L^2\Lambda^{n-q}_{\Gamma_1} \times \cdots \times L^2\Lambda^{n-q}_{\Gamma_{n_\Gamma}} \times L^2\Lambda^{n-p}_{\hat{\Gamma}_1} \times \cdots \times L^2\Lambda^{n-p}_{\hat{\Gamma}_{\hat{n}_\Gamma}}
\end{aligned}
\tag{31}
$$

where

$$
\begin{aligned}
\langle v^p | f^p \rangle_\Omega &= \langle v^p | (-1)^r \mathrm{d} e^q \rangle_\Omega \qquad && \forall v^p \in H^1\Lambda^{n-p}(\Omega), \\
\langle v^q | f^q \rangle_\Omega &= \langle v^q | \mathrm{d} e^p \rangle_\Omega && \forall v^q \in H^1\Lambda^{n-q}(\Omega),
\end{aligned}
\tag{32}
$$

and

$$
\begin{aligned}
f_i^\Gamma &= \mathrm{tr}_{\Gamma_i} e^p, \qquad & \hat{f}_j^\Gamma &= (-1)^p \mathrm{tr}_{\hat{\Gamma}_j} e^q, \\
e_i^\Gamma &= (-1)^p \,\mathrm{tr}_{\Gamma_i} e^q, & \hat{e}_j^\Gamma &= \mathrm{tr}_{\hat{\Gamma}_j} e^p.
\end{aligned}
\tag{33}
$$

Remark 4. Note the subtle *formal* difference in the definition of the boundary port variables. In (25) they are defined as restrictions of the *smooth* effort forms to the boundary, uniquely defined by continuity. Here, we use the *trace* operator, which defines the extension of an H^1 form to the boundary, see Appendix **??**.

[19] By using a *discrete variational formulation* space-time discrete models can be even obtained directly, see e.g. [41].

[20] The paper is a good introduction to exterior differential calculus.

[21] In the variational formulation of boundary value problems, mostly test functions with compact support inside Ω are chosen such that boundary conditions have to be imposed *directly* on the solution. This is however, not mandatory. By test functions which are non-zero on $\partial\Omega$, boundary conditions can be imposed in a *weak* fashion, cf. [47], Section 14.3.1, p. 483.

[22] For brevity, the domain of the differential forms is written as an index, e.g. $L^2\Lambda^p_\Omega = L^2\Lambda^p_\Omega$.

With the functional spaces of the flow and effort differential forms $(f^p, f^q, f_1^\Gamma, \dots, f_{n_\Gamma}^\Gamma, \hat{f}_1^\Gamma, \dots, \hat{f}_{\hat{n}_\Gamma}^\Gamma)$ and $(e^p, e^q, e_1^\Gamma, \dots, e_{n_\Gamma}^\Gamma, \hat{e}_1^\Gamma, \dots, \hat{e}_{\hat{n}_\Gamma}^\Gamma)$ integration by parts according to (**??**) is applicable, which yields the following weak form of the Stokes-Dirac structure.

Proposition 2. *The* weak *form of the Stokes-Dirac structure in Prop. 1 with* weak *treatment of boundary port variables is given by the subset $D \subset \mathcal{F} \times \mathcal{E}$, $\mathcal{F}$ and $\mathcal{E}$ according to* (31)*, where*

$$\begin{aligned} \langle v^p | f^p \rangle_\Omega &= (-1)^{r+q} \langle \mathrm{d} v^p | e^q \rangle_\Omega - (-1)^{r+p+q} \sum_{i=1}^{n_\Gamma} \langle \operatorname{tr} v^p | e_i^\Gamma \rangle_{\Gamma_i} - (-1)^{r+p+q} \sum_{j=1}^{\hat{n}_\Gamma} \langle \operatorname{tr} v^p | \hat{f}_j^\Gamma \rangle_{\hat{\Gamma}_j} \\ \langle v^q | f^q \rangle_\Omega &= (-1)^{p} \langle \mathrm{d} v^q | e^p \rangle_\Omega - (-1)^{p} \sum_{i=1}^{n_\Gamma} \langle \operatorname{tr} v^q | f_i^\Gamma \rangle_{\Gamma_i} - (-1)^{p} \sum_{j=1}^{\hat{n}_\Gamma} \operatorname{tr} \langle v^q | \hat{e}_j^\Gamma \rangle_{\hat{\Gamma}_j}, \end{aligned} \tag{34}$$

holds for all test forms $v^p \in H^1\Lambda^{n-p}(\Omega)$ and $v^q \in H^1\Lambda^{n-q}(\Omega)$.

Proof. Eq. (34) follows from (32) via integration by parts and the identities

$$\begin{aligned} (-1)^p \langle v^p | \operatorname{tr} e^q \rangle_{\partial\Omega} &= \sum_{i=1}^{n_\Gamma} \langle v^p | e_i^\Gamma \rangle_{\Gamma_i} + \sum_{j=1}^{\hat{n}_\Gamma} \langle v^p | \hat{f}_j^\Gamma \rangle_{\hat{\Gamma}_j}, \\ \langle v^q | \operatorname{tr} e^p \rangle_{\partial\Omega} &= \sum_{i=1}^{n_\Gamma} \langle v^q | f_i^\Gamma \rangle_{\Gamma_i} + \sum_{j=1}^{\hat{n}_\Gamma} \langle v^q | \hat{e}_j^\Gamma \rangle_{\hat{\Gamma}_j}. \end{aligned} \tag{35}$$

The latter are due to the definition (33) of boundary port variables and the definition of the subsets Γ_i, $\hat{\Gamma}_j$ which cover completely $\partial\Omega$ and whose intersections are either empty or have dimension $n-1$. ☐

Remark 5. The latter representation of the Stokes-Dirac structure – if considered on a single control volume – is suitable for *discontinuous Galerkin* schemes, see e.g. [32], where the boundary terms are replaced by suitable *numerical fluxes.*

Using the effort forms as test forms, $v^p = e^p$, $v^q = e^q$, and adding both equations of (34), we obtain (after some reformulations and exploiting (28), see appendix)

$$\langle e^p | f^p \rangle_\Omega + \langle e^q | f^q \rangle_\Omega + (-1)^p \langle e^q | e^p \rangle_{\partial\Omega} = 0, \tag{36}$$

or, with the definition of boundary port variables,

$$\langle e^p | f^p \rangle_\Omega + \langle e^q | f^q \rangle_\Omega + \sum_{\mu=1}^{n_\Gamma} \langle e^{\partial,\mu} | f^{\partial,\mu} \rangle_{\Gamma_\mu} + \sum_{\nu=1}^{\hat{n}_\Gamma} \langle \hat{f}^{\partial,\nu} | \hat{e}^{\partial,\nu} \rangle_{\hat{\Gamma}_\nu} = 0, \tag{37}$$

which corresponds to the initially derived power continuity equation (17).

We have arrived at a weak (or variational) representation of the Stokes-Dirac structure of Prop. (1) which suits to establish discretized mixed Galerkin models of PH systems of two conservation laws.

3.2 Mixed Galerkin approximation

In this section, we introduce the mixed Galerkin approximation of the weak form of the Stokes-Dirac structure for a system of two conservation laws. For convenience of notation, we omit to explicitly write out the trace operator on the subsets of the boundary, i.e. $\langle v^p | e^q \rangle_{\Gamma_i} := \langle \operatorname{tr} v^p | \operatorname{tr} e^q \rangle_{\Gamma_i}$ etc. in the sequel. We start with the representation

$$\begin{aligned} \langle v^p | f^p \rangle_\Omega &= (-1)^{r+q} \langle \mathrm{d} v^p | e^q \rangle_\Omega - (-1)^{r+q} \sum_{i=1}^{n_\Gamma} \langle v^p | e^q \rangle_{\Gamma_i} - (-1)^{r+q} \sum_{j=1}^{\hat{n}_\Gamma} \langle v^p | e^q \rangle_{\hat{\Gamma}_j} \\ \langle v^q | f^q \rangle_\Omega &= (-1)^{p} \langle \mathrm{d} v^q | e^p \rangle_\Omega - (-1)^{p} \sum_{i=1}^{n_\Gamma} \langle v^q | e^p \rangle_{\Gamma_i} - (-1)^{p} \sum_{j=1}^{\hat{n}_\Gamma} \langle v^q | e^p \rangle_{\hat{\Gamma}_j}, \end{aligned} \tag{38}$$

i.e. (34) without the explicit denomination of the boundary port variables. For a *mixed Galerkin* approximation of the Stokes-Dirac structure, we

- use different (*mixed*) bases to approximate the spaces of flow and effort forms
- and, from these bases, we choose the appropriate ones to approximate the test forms (*Galerkin* method).

For the Stokes-Dirac structure, the effort bases are the natural choice to approximate the spaces of test forms, as they retain the interpretation of the duality products as power products, see (36).

Note that from the original (strong) formulation of the Stokes-Dirac structure, until its weak formulation, both equations feature only the exterior derivative and *not* the co-differential, i.e. no information about the *metric* on the functional spaces is contained. Nor do we decide – for a finite-element (FE) discretization which serves as illustrative example – to approximate the two equations on different, staggered grids, as it is common practice in computational electromagnetism [12] or the numerical treatment of transport phenomena [44]. Instead, we approximate the variables in both conservation laws with the same conforming subspaces (i.e. on the same mesh in FE), which has the advantage that boundary variables are defined directly *on* $\partial\Omega$, without having to cope with an eventual grid shift.

Nevertheless, the power-preserving maps that will be introduced to ensure *non-degenerate* duality pairings between the discrete bond variables will give rise to an interpretation of the resulting schemes in terms of staggered grids by the localization of the mapped discrete variables. The ability to *parametrize* the power-preserving maps will allow to adapt the approximation to the nature of the system, e.g. to account for diffusive effects in a hyperbolic system.

3.2.1 Approximation problem and compatibility condition

The flow differential forms will be approximated by linear combinations of appropriate basis forms of subspaces

$$\begin{array}{rclcl} \Psi_h^p & = & \mathrm{span}\{\psi_1^p, \ldots, \psi_{N_p}^p\} & \subset & L^2\Lambda^p(\Omega) \\ \Psi_h^q & = & \mathrm{span}\{\psi_1^p, \ldots, \psi_{N_q}^q\} & \subset & L^2\Lambda^q(\Omega). \end{array} \tag{39}$$

The subspaces for the effort and test forms are, accordingly,

$$\begin{array}{rclcl} \Phi^p & = & \mathrm{span}\{\varphi_1^p, \ldots, \varphi_{M_p}^p\} & \subset & H^1\Lambda^{n-p}(\Omega) \\ \Phi_h^q & = & \mathrm{span}\{\varphi_1^q, \ldots, \varphi_{M_q}^q\} & \subset & H^1\Lambda^{n-q}(\Omega). \end{array} \tag{40}$$

From the trace theorem for H^1 spaces (see Appendix **??**), we know that the restriction of the latter spaces to the boundary is L^2. $h > 0$ denotes the discretization parameter[23] and we assume an *appropriate* choice of approximation spaces, i.e. for a given functional space V and its approximation V_h (see [47], Section 5.2) it is true that $\inf_{v_h \in V_h} \|v - v_h\| \to 0$ for all $v \in V$ if $h \to 0$. The *mixed Galerkin approximation problem* is as follows: Find approximate flow and effort forms

$$\begin{aligned} f_h^p(\mathbf{z}) &= \sum_{k=1}^{N_p} f_k^p \psi_k^p(\mathbf{z}) = \langle \mathbf{f}^p, \boldsymbol{\psi}^p(\mathbf{z}) \rangle \in \Psi_h^p, \\ f_h^q(\mathbf{z}) &= \sum_{l=1}^{N_q} f_l^q \psi_l^q(\mathbf{z}) = \langle \mathbf{f}^q, \boldsymbol{\psi}^q(\mathbf{z}) \rangle \in \Psi_h^q, \end{aligned} \tag{41}$$

and

$$\begin{aligned} e_h^p(\mathbf{z}) &= \sum_{i=1}^{M_p} e_i^p \varphi_i^p(\mathbf{z}) = \langle \mathbf{e}^p, \boldsymbol{\varphi}^p(\mathbf{z}) \rangle \in \Phi_h^p, \\ e_h^q(\mathbf{z}) &= \sum_{j=1}^{M_q} e_j^q \varphi_j^q(\mathbf{z}) = \langle \mathbf{e}^q, \boldsymbol{\varphi}^q(\mathbf{z}) \rangle \in \Phi_h^q, \end{aligned} \tag{42}$$

[23] Which corresponds to the spatial extent of finite elements or the reciprocal order of a polynomial approximation.

where $\langle \cdot, \cdot \rangle$ denotes the standard inner product in $\mathbb{R}^n$, such that

$$
\begin{aligned}
\langle v_h^p | f_h^p \rangle_\Omega &= (-1)^{r+q} \langle \mathrm{d} v_h^p | e_h^q \rangle_\Omega - (-1)^{r+q} \sum_{\mu=1}^{n_\Gamma} \langle v_h^p | e_h^q \rangle_{\Gamma_\mu} - (-1)^{r+q} \sum_{\nu=1}^{\hat{n}_\Gamma} \langle v_h^p | e_h^q \rangle_{\hat{\Gamma}_\nu} \\
\langle v_h^q | f_h^q \rangle_\Omega &= (-1)^{p} \langle \mathrm{d} v_h^q | e_h^p \rangle_\Omega - (-1)^{p} \sum_{\mu=1}^{n_\Gamma} \langle v_h^q | e_h^p \rangle_{\Gamma_\mu} - (-1)^{p} \sum_{\nu=1}^{\hat{n}_\Gamma} \langle v_h^q | e_h^p \rangle_{\hat{\Gamma}_\nu}.
\end{aligned} \tag{43}
$$

holds for all $v_h^p \in \Phi_h^p$, $v_h^q \in \Phi_h^q$. The *discrete flow and effort vectors*

$$
\begin{aligned}
\mathbf{f}^p &= [f_1^p, \ldots, f_{N_p}^p]^T, \\
\mathbf{f}^q &= [f_1^q, \ldots, f_{N_q}^q]^T,
\end{aligned}
\quad \text{and} \quad
\begin{aligned}
\mathbf{e}^p &= [e_1^p, \ldots, e_{M_p}^p]^T, \\
\mathbf{e}^q &= [e_1^q, \ldots, e_{M_q}^q]^T,
\end{aligned} \tag{44}
$$

contain the approximation coefficients, and the vectors (we omit the argument $\mathbf{z}$ in the sequel)

$$
\begin{aligned}
\boldsymbol{\psi}^p(\mathbf{z}) &= [\psi_1^p(\mathbf{z}), \ldots, \psi_{N_p}^p(\mathbf{z})]^T, \\
\boldsymbol{\psi}^q(\mathbf{z}) &= [\psi_1^q(\mathbf{z}), \ldots, \psi_{N_q}^q(\mathbf{z})]^T,
\end{aligned}
\quad \text{and} \quad
\begin{aligned}
\boldsymbol{\varphi}^p(\mathbf{z}) &= [\varphi_1^p(\mathbf{z}), \ldots, \varphi_{M_p}^p(\mathbf{z})]^T, \\
\boldsymbol{\varphi}^q(\mathbf{z}) &= [\varphi_1^q(\mathbf{z}), \ldots, \varphi_{M_q}^q(\mathbf{z})]^T,
\end{aligned} \tag{45}
$$

contain the approximation basis forms.

The flow variables are understood as time derivatives of the distributed states with negative sign, see (15). Thus, they are approximated with the same bases,

$$
\begin{aligned}
p_h(\mathbf{z}) &= \sum_{k=1}^{N_p} p_k \psi_k^p(\mathbf{z}) = \langle \mathbf{p}, \boldsymbol{\psi}^p(\mathbf{z}) \rangle \in \Psi_h^p, \\
q_h(\mathbf{z}) &= \sum_{l=1}^{N_q} q_l \psi_l^q(\mathbf{z}) = \langle \mathbf{q}, \boldsymbol{\psi}^q(\mathbf{z}) \rangle \in \Psi_h^q,
\end{aligned} \tag{46}
$$

and

$$
\mathbf{p} = [p_1, \ldots, p_{N_p}]^T \quad \text{and} \quad \mathbf{q} = [q_1, \ldots, q_{N_q}]^T. \tag{47}
$$

denote the *discrete state vectors*.

The mixed Galerkin approximation (43) of (38) is *exact* for flow and effort forms from the approximation spaces (39), (40) (in these subspaces, the residual error vanishes), if the following *compatibility conditions* hold:

$$
\begin{aligned}
\operatorname{span}\{\psi_1^p, \ldots, \psi_{N_p}^p\} &= \operatorname{span}\{\mathrm{d}\varphi_1^q, \ldots, \mathrm{d}\varphi_{M_q}^q\} \\
\operatorname{span}\{\psi_1^q, \ldots, \psi_{N_q}^q\} &= \operatorname{span}\{\mathrm{d}\varphi_1^p, \ldots, \mathrm{d}\varphi_{M_p}^p\}.
\end{aligned} \tag{48}
$$

In contrast to [29] (Assumptions 3 and 7), this *compatibility of forms* is understood *in the weak sense*. This means, more precisely – consider the original weak formulation (32) and the definition of the weak exterior derivative – that for all test forms with compact support inside Ω, i.e. $v^p \in H_0^1 \Lambda^{n-p}(\Omega)$, $v^q \in H_0^1 \Lambda^{n-q}(\Omega)$, there exist constants a_k^p, a_l^q, b_i^p, b_j^q such that

$$
\begin{aligned}
\sum_{k=1}^{N_p} a_k^p \langle v^p | \psi_k^p \rangle_\Omega + \sum_{j=1}^{M_q} b_j^q \langle v^p | \mathrm{d}\varphi_j^q \rangle_\Omega = 0, \\
\sum_{l=1}^{N_q} a_l^q \langle v^q | \psi_l^q \rangle_\Omega + \sum_{i=1}^{M_p} b_i^p \langle v^q | \mathrm{d}\varphi_i^p \rangle_\Omega = 0.
\end{aligned} \tag{49}
$$

3.2.2 Approximation of the variational problem

The weak formulation (38) of the Stokes-Dirac structure represents a *variational problem*: flow and effort forms are sought under arbitrary variation of the test forms. Replacing the finite-dimensional approximations (41), (42) and using the test forms from the effort bases,

$$
v_h^p = \langle \mathbf{v}^p, \boldsymbol{\varphi}^p \rangle, \quad v_h^q = \langle \mathbf{v}^q, \boldsymbol{\varphi}^q \rangle, \qquad \mathbf{v}^p \in \mathbb{R}^{M_p}, \ \mathbf{v}^q \in \mathbb{R}^{M_q}, \tag{50}
$$

we obtain the equations (the exterior derivative applies element-wise to a vector of differential forms)

$$\begin{aligned}\Big\langle \langle \mathbf{v}^p, \boldsymbol{\varphi}^p\rangle \,\Big|\, \langle \mathbf{f}^p, \boldsymbol{\psi}^p\rangle \Big\rangle_\Omega - (-1)^{r+q}\Big\langle \langle \mathbf{v}^p, \mathrm{d}\boldsymbol{\varphi}^p\rangle \,\Big|\, \langle \mathbf{e}^q, \boldsymbol{\varphi}^q\rangle \Big\rangle_\Omega \\ + (-1)^{r+q}\sum_{\mu=1}^{n_\Gamma} \Big\langle \langle \mathbf{v}^p, \boldsymbol{\varphi}^p\rangle \,\Big|\, \langle \mathbf{e}^q, \boldsymbol{\varphi}^q\rangle \Big\rangle_{\Gamma_\mu} + (-1)^{r+q}\sum_{\nu=1}^{\hat{n}_\Gamma} \Big\langle \langle \mathbf{v}^p, \boldsymbol{\varphi}^p\rangle \,\Big|\, \langle \mathbf{e}^q, \boldsymbol{\varphi}^q\rangle \Big\rangle_{\hat{\Gamma}_\nu} = 0\end{aligned} \tag{51}$$

and

$$\begin{aligned}\Big\langle \langle \mathbf{v}^q, \boldsymbol{\varphi}^q\rangle \,\Big|\, \langle \mathbf{f}^q, \boldsymbol{\psi}^q\rangle \Big\rangle_\Omega - (-1)^{p}\Big\langle \langle \mathbf{v}^q, \mathrm{d}\boldsymbol{\varphi}^q\rangle \,\Big|\, \langle \mathbf{e}^p, \boldsymbol{\varphi}^p\rangle \Big\rangle_\Omega \\ + (-1)^{p}\sum_{\mu=1}^{n_\Gamma} \Big\langle \langle \mathbf{v}^q, \boldsymbol{\varphi}^q\rangle \,\Big|\, \langle \mathbf{e}^p, \boldsymbol{\varphi}^p\rangle \Big\rangle_{\Gamma_\mu} + (-1)^{p}\sum_{\nu=1}^{\hat{n}_\Gamma} \Big\langle \langle \mathbf{v}^q, \boldsymbol{\varphi}^q\rangle \,\Big|\, \langle \mathbf{e}^p, \boldsymbol{\varphi}^p\rangle \Big\rangle_{\hat{\Gamma}_\nu} = 0\end{aligned} \tag{52}$$

Evaluating the integrals over the basis forms, we get the short notation of the *finite dimensional variatonal problem*

$$\begin{aligned}\Big\langle \mathbf{v}^p, \mathbf{M}_p\mathbf{f}^p\Big\rangle + \Big\langle \mathbf{v}^p, \Big(\mathbf{K}_p + \sum_{\mu=1}^{n_\Gamma}\mathbf{L}_p^\mu + \sum_{\nu=1}^{\hat{n}_\Gamma}\hat{\mathbf{L}}_p^\nu\Big)\mathbf{e}^q\Big\rangle = 0 \qquad \forall \mathbf{v}^p \in \mathbb{R}^{M_p}, \\ \Big\langle \mathbf{v}^q, \mathbf{M}_q\mathbf{f}^q\Big\rangle + \Big\langle \mathbf{v}^q, \Big(\mathbf{K}_q + \sum_{\mu=1}^{n_\Gamma}\mathbf{L}_q^\mu + \sum_{\nu=1}^{\hat{n}_\Gamma}\hat{\mathbf{L}}_q^\nu\Big)\mathbf{e}^q\Big\rangle = 0 \qquad \forall \mathbf{v}^q \in \mathbb{R}^{M_q}.\end{aligned} \tag{53}$$

whose matrices $\mathbf{M}_p \in \mathbb{R}^{M_p\times N_p}$, $\mathbf{M}_q \in \mathbb{R}^{M_q\times N_q}$, $\mathbf{K}_p, \mathbf{L}_p^\mu, \hat{\mathbf{L}}_p^\nu \in \mathbb{R}^{M_p\times M_q}$, $\mathbf{K}_q, \mathbf{L}_q^\mu, \hat{\mathbf{L}}_q^\nu \in \mathbb{R}^{M_q\times M_p}$, $\mu = 1,\ldots,n_\Gamma$, $\nu = 1,\ldots,\hat{n}_\Gamma$, are composed of the elements

$$\begin{array}{rclrcl} [\mathbf{M}_p]_{ik} &=& \langle \varphi_i^p|\psi_k^p\rangle_\Omega, & [\mathbf{M}_q]_{jl} &=& \langle \varphi_j^q|\psi_l^q\rangle_\Omega, \\ [\mathbf{K}_p]_{ij} &=& -(-1)^{r+q}\langle \mathrm{d}\varphi_i^p|\varphi_j^q\rangle_\Omega, & [\mathbf{K}_q]_{ji} &=& -(-1)^{p}\langle \mathrm{d}\varphi_j^q|\varphi_i^p\rangle_\Omega, \\ [\mathbf{L}_p^\mu]_{ij} &=& (-1)^{r+q}\langle \varphi_i^p|\varphi_j^q\rangle_{\Gamma_\mu}, & [\mathbf{L}_q^\mu]_{ji} &=& (-1)^{p}\langle \varphi_j^q|\varphi_i^p\rangle_{\Gamma_\mu}, \\ [\hat{\mathbf{L}}_p^\nu]_{ij} &=& (-1)^{r+q}\langle \varphi_i^p|\varphi_j^q\rangle_{\hat{\Gamma}_\nu}, & [\hat{\mathbf{L}}_q^\nu]_{ji} &=& (-1)^{p}\langle \varphi_j^q|\varphi_i^p\rangle_{\hat{\Gamma}_\nu}. \end{array} \tag{54}$$

Equations (53) must hold for arbitrary vectors (discrete variations) $\mathbf{v}^p$, $\mathbf{v}^q$, which gives the matrix equations

$$\begin{aligned}\mathbf{M}_p\mathbf{f}^p + (\mathbf{K}_p + \mathbf{L}_p)\mathbf{e}^q = \mathbf{0}, \\ \mathbf{M}_q\mathbf{f}^q + (\mathbf{K}_q + \mathbf{L}_q)\mathbf{e}^p = \mathbf{0}.\end{aligned} \tag{55}$$

It is straightforward to show by application of (**??**) that

$$[\mathbf{L}_p^\mu]_{ij} = [\mathbf{L}_q^\mu]_{ji}, \qquad [\hat{\mathbf{L}}_p^\nu]_{ij} = [\hat{\mathbf{L}}_q^\mu]_{ji} \tag{56}$$

i.e. $\mathbf{L}_p^\mu = (\mathbf{L}_q^\mu)^T$ and $\hat{\mathbf{L}}_p^\nu = (\hat{\mathbf{L}}_q^\nu)^T$. By defining

$$\mathbf{L}_p = \sum_{\mu=1}^{n_\Gamma}\mathbf{L}_p^\mu + \sum_{\nu=1}^{\hat{n}_\Gamma}\hat{\mathbf{L}}_p^\nu, \qquad \mathbf{L}_q = \sum_{\mu=1}^{n_\Gamma}\mathbf{L}_q^\mu + \sum_{\nu=1}^{\hat{n}_\Gamma}\hat{\mathbf{L}}_q^\nu, \tag{57}$$

we can prove the following.

Proposition 3. *The following relation holds between the elements of the matrices $\mathbf{K}_p, \mathbf{K}_q$ and $\mathbf{L}_p, \mathbf{L}_q$.*

$$[\mathbf{K}_p + \mathbf{L}_p]_{ij} + [\mathbf{K}_q + \mathbf{L}_q]_{ji} = [\mathbf{L}_p]_{ij} = [\mathbf{L}_q]_{ji}, \tag{58}$$

i.e. $(\mathbf{K}_p + \mathbf{L}_p) + (\mathbf{K}_q + \mathbf{L}_q)^T = \mathbf{L}_p = \mathbf{L}_q^T$.

Proof. By the definition (57), the elements of $\mathbf{L}_p, \mathbf{L}_q$ are duality products over the effort basis forms on the complete boundary $\partial\Omega$. Thus, we have that

$$[\mathbf{K}_p + \mathbf{L}_p]_{ij} + [\mathbf{K}_q + \mathbf{L}_q]_{ji} = \\ -(-1)^{r+q}\langle \mathrm{d}\varphi_i^p | \varphi_j^q\rangle_\Omega + (-1)^{r+q}\langle \varphi_i^p | \varphi_j^q\rangle_{\partial\Omega} - (-1)^p\langle \mathrm{d}\varphi_j^q | \varphi_i^p\rangle_\Omega + (-1)^p\langle \varphi_j^q | \varphi_i^p\rangle_{\partial\Omega}. \quad (59)$$

Using skew-symmetry of the wedge product and the integration-by-parts formula for differential forms, the right hand side can be rewritten as

$$(-1)^p\langle \varphi_j^q(z) | \varphi_i^p(z)\rangle_{\partial\Omega} = [\mathbf{L}_q]_{ji} = [\mathbf{L}_p]_{ij}, \quad (60)$$

which completes the proof. □

Proposition 4. *The finite-dimensional approximation of the power continuity equation* (36) *is*

$$\langle \mathbf{e}^p, \mathbf{M}_p\mathbf{f}^p\rangle + \langle \mathbf{e}^q, \mathbf{M}_q\mathbf{f}^q\rangle + \langle \mathbf{e}^q, \mathbf{L}_q\mathbf{e}^p\rangle = 0 \quad (61a)$$

or

$$\langle \mathbf{e}^p, \mathbf{M}_p\mathbf{f}^p\rangle + \langle \mathbf{e}^q, \mathbf{M}_q\mathbf{f}^q\rangle + \langle \mathbf{L}_p\mathbf{e}^q, \mathbf{e}^p\rangle = 0, \quad (61b)$$

where $\langle\cdot,\cdot\rangle$ *denotes the standard inner product on Euclidean space.*

Proof. The relations follow from replacing $\mathbf{v}^p = \mathbf{e}^p$, $\mathbf{v}^q = \mathbf{e}^q$ in the finite-dimensional variational problem (53), adding both equations, substituting the definition (57) of $\mathbf{L}_p$, $\mathbf{L}_q$, and exploiting the property (58). □

As the matrices $\mathbf{L}_p, \mathbf{L}_p^\mu, \hat{\mathbf{L}}_p^\nu$ and $\mathbf{L}_q, \mathbf{L}_q^\mu, \hat{\mathbf{L}}_q^\nu$ describe the approximate power transferred over the boundary $\partial\Omega$ or parts of it, we refer to them as them *boundary power matrices.* $\mathbf{L}_p = \mathbf{L}_q^T$, whose elements are the integrals of duality pairings between approximation forms on the boundary, will have reduced rank. The reason is that basis forms for interior effort degrees of freedom will be, in general, zero on the boundary[24].

3.2.3 Discrete boundary port variables

In the next step, we characterize mappings to *discrete boundary port variables*, according to the subdivision of the boundary $\partial\Omega$ into disjoint regions Γ_i, $i = 1,\dots,n_\Gamma$, $\hat{\Gamma}_j$, $j = 1,\dots,\hat{n}_\Gamma$. These subsets of the discrete effort variables will be assigned either the role of discrete boundary in- or outputs.

Definition 4. The vectors of *discrete boundary port variables*[25] $\mathbf{e}^{b,\mu}, \mathbf{f}_0^{b,\mu} \in \mathbb{R}^{M_b^\mu}$ and $\hat{\mathbf{e}}^{b,\nu}, \hat{\mathbf{f}}_0^{b,\nu} \in \mathbb{R}^{\hat{M}_b^\nu}$, associated with the boundary subdomains $\Gamma_\mu \subset \partial\Omega$, $\mu = 1,\dots,n_\Gamma$, $\hat{\Gamma}_\nu \subset \partial\Omega$, $\nu = 1,\dots,\hat{n}_\Gamma$ are defined via the discrete expression of the power transfered over Γ_μ and $\hat{\Gamma}_\nu$, respectively:

$$\langle \mathbf{e}^q, \mathbf{L}_q^\mu\mathbf{e}^p\rangle =: \langle \mathbf{e}^{b,\mu}, \mathbf{f}_0^{b,\mu}\rangle, \qquad \langle \mathbf{e}^p, \hat{\mathbf{L}}_p^\nu\mathbf{e}^q\rangle =: \langle \hat{\mathbf{e}}^{b,\nu}, \hat{\mathbf{f}}_0^{b,\nu}\rangle. \quad (62)$$

We decompose the boundary power matrices for each boundary subdomain in matrix products

$$\mathbf{L}_q^\mu = (\mathbf{T}_q^\mu)^T\mathbf{S}_{p,0}^\mu, \qquad \hat{\mathbf{L}}_p^\nu = (\hat{\mathbf{T}}_p^\nu)^T\hat{\mathbf{S}}_{q,0}^\nu. \quad (63)$$

The *boundary trace matrices*[26] $\mathbf{T}_q^\mu \in \mathbb{R}^{M_b^\mu \times M_q}$, $\hat{\mathbf{T}}_p^\nu \in \mathbb{R}^{\hat{M}_b^\nu \times M_p}$ define the effort degrees of freedom

$$\mathbf{e}^{b,\mu} = \mathbf{T}_q^\mu\mathbf{e}^q, \qquad \hat{\mathbf{e}}^{b,\nu} = \hat{\mathbf{T}}_p^\nu\mathbf{e}^p. \quad (64)$$

that lie on the boundary and are assigned the roles of *input variables.* We call $\mathbf{S}_{p,0}^\mu \in \mathbb{R}^{M_b^\mu \times M_p}$, $\hat{\mathbf{S}}_{q,0}^\nu \in \mathbb{R}^{\hat{M}_b^\nu \times M_q}$ the *collocated boundary output* matrices. They define the boundary flow variables

$$\mathbf{f}_0^{b,\mu} = \mathbf{S}_{p,0}^\mu\mathbf{e}^p, \qquad \hat{\mathbf{f}}_0^{b,\nu} = \hat{\mathbf{S}}_{q,0}^\nu\mathbf{e}^q, \quad (65)$$

which, together with the discrete efforts (64), satisfy exactly the discrete power balance (62) on the different portions of the boundary.

[24] This is definitely true for finite elements, which are the standard Galerkin approximation in more than one spatial dimension. Also for the 1D pseudo-spectral collocation method, see [42].

[25] Discrete boundary variables have index b, in contrast to index ∂ for the original distributed quantities.

[26] This denomination refers to the trace theorem that clarifies the functional space of H^1 functions *restricted to* (a subset of) the boundary.

Because of

$$\begin{aligned}\langle e^{\partial,\mu}|f^{\partial,\mu}\rangle_{\Gamma_\mu} &= (-1)^p\langle e^q|e^p\rangle_{\Gamma_\mu} \approx (-1)^p\Big\langle\langle \mathbf{e}^q,\boldsymbol{\varphi}^q\rangle\Big|\langle \mathbf{e}^p,\boldsymbol{\varphi}^p\rangle\Big\rangle_{\Gamma_\mu} = \langle \mathbf{e}^q,\mathbf{L}_q^\mu \mathbf{e}^p\rangle = \langle \mathbf{e}^{b,\mu},\mathbf{f}_0^{b,\mu}\rangle,\\ \langle \hat{e}^{\partial,\nu}|\hat{f}^{\partial,\nu}\rangle_{\hat{\Gamma}_\nu} &= (-1)^p\langle e^p|e^q\rangle_{\hat{\Gamma}_\nu} \approx (-1)^p\Big\langle\langle \mathbf{e}^p,\boldsymbol{\varphi}^p\rangle\Big|\langle \mathbf{e}^q,\boldsymbol{\varphi}^q\rangle\Big\rangle_{\hat{\Gamma}_\nu} = \langle \mathbf{e}^p,\hat{\mathbf{L}}_p^\nu \mathbf{e}^q\rangle = \langle \hat{\mathbf{e}}^{b,\nu},\hat{\mathbf{f}}_0^{b,\nu}\rangle,\end{aligned} \tag{66}$$

the definition of discrete boundary port variables is consistent with the distributed definition (33). Summation over the individual boundary power matrices according to (57), yields the boundary power balance in compact notation

$$\mathbf{T}_q^T\mathbf{S}_{p,0} + \hat{\mathbf{S}}_{q,0}^T\hat{\mathbf{T}}_p = \mathbf{L}_q, \tag{67}$$

where

$$\mathbf{T}_q = \begin{bmatrix}\mathbf{T}_q^1\\ \vdots\\ \mathbf{T}_q^{n_\Gamma}\end{bmatrix},\quad \mathbf{S}_{p,0} = \begin{bmatrix}\mathbf{S}_{p,0}^1\\ \vdots\\ \mathbf{S}_{p,0}^{n_\Gamma}\end{bmatrix},\qquad \hat{\mathbf{S}}_{q,0} = \begin{bmatrix}\hat{\mathbf{S}}_{q,0}^1\\ \vdots\\ \hat{\mathbf{S}}_{q,0}^{\hat{n}_\Gamma}\end{bmatrix},\quad \hat{\mathbf{T}}_p = \begin{bmatrix}\hat{\mathbf{T}}_p^1\\ \vdots\\ \hat{\mathbf{T}}_p^{\hat{n}_\Gamma}\end{bmatrix}. \tag{68}$$

The discrete power continuity equation, which represents the counterpart of (37) *in the approximation subspaces*, finally reads

$$\langle \mathbf{e}^p,\mathbf{M}_p\mathbf{f}^p\rangle + \langle \mathbf{e}^q,\mathbf{M}_q\mathbf{f}^q\rangle + \langle \mathbf{e}^b,\mathbf{f}_0^b\rangle + \langle \hat{\mathbf{e}}^b,\hat{\mathbf{f}}_0^b\rangle = 0, \tag{69}$$

where the vectors

$$\mathbf{e}^b = \begin{bmatrix}\mathbf{e}^{b,1}\\ \vdots\\ \mathbf{e}^{b,n_\Gamma}\end{bmatrix},\quad \mathbf{f}_0^b = \begin{bmatrix}\mathbf{f}_0^{b,1}\\ \vdots\\ \mathbf{f}_0^{b,n_\Gamma}\end{bmatrix},\qquad \hat{\mathbf{e}}^b = \begin{bmatrix}\mathbf{e}^{b,1}\\ \vdots\\ \mathbf{e}^{b,\hat{n}_\Gamma}\end{bmatrix},\quad \hat{\mathbf{f}}_0^b = \begin{bmatrix}\mathbf{f}_0^{b,1}\\ \vdots\\ \mathbf{f}_0^{b,\hat{n}_\Gamma}\end{bmatrix}. \tag{70}$$

satisfy

$$\mathbf{e}^b = \mathbf{T}_q\mathbf{e}^q,\quad \mathbf{f}_0^b = \mathbf{S}_{p,0}\mathbf{e}^p,\qquad \hat{\mathbf{e}}^b = \hat{\mathbf{T}}_p\mathbf{e}^p,\quad \hat{\mathbf{f}}_0^b = \hat{\mathbf{S}}_{q,0}\mathbf{e}^q. \tag{71}$$

We are at the point to express the subspace of the discrete bond space on which power continuity according to (69) holds, corresponding to the infinite-dimensional Stokes-Dirac structure in Prop. 1:

Proposition 5. *Given the finite-dimensional space of discrete flows and efforts*

$$\mathcal{F}\times\mathcal{E} = \mathbb{R}^{N_p}\times\mathbb{R}^{N_q}\times\mathbb{R}^{M_b}\times\mathbb{R}^{\hat{M}_b}\times\mathbb{R}^{M_p}\times\mathbb{R}^{M_q}\times\mathbb{R}^{M_b}\times\mathbb{R}^{\hat{M}_b} \tag{72}$$

with $M_b = \sum_{\mu=1}^{n_\Gamma} M_b^\mu$, $\hat{M}_b = \sum_{\nu=1}^{\hat{n}_\Gamma}\hat{M}_b^\nu$. *The subspace*

$$\{(\mathbf{f}^p,\mathbf{f}^q,\mathbf{f}_0^b,\hat{\mathbf{f}}_0^b,\mathbf{e}^p,\mathbf{e}^q,\mathbf{e}^b,\hat{\mathbf{e}}^b)\in\mathcal{F}\times\mathcal{E}\mid (53)\ \textit{and}\ (64),(65)\ \textit{hold}\} \tag{73}$$

satisfies the isotropy[27] condition, $D\subset D^\perp$ *with respect to the bilinear form* $\langle\langle\cdot,\cdot\rangle\rangle_M$ *that results from symmetrization of the* degenerate *duality product*

$$\langle\cdot,\cdot\rangle_M := \langle \mathbf{e}^p,\mathbf{M}_p\mathbf{f}^p\rangle + \langle \mathbf{e}^q,\mathbf{M}_q\mathbf{f}^q\rangle + \langle \mathbf{e}^b,\mathbf{f}_0^b\rangle + \langle \hat{\mathbf{e}}^b,\hat{\mathbf{f}}_0^b\rangle. \tag{74}$$

Proof. Along the lines of Prop. 18 in [42]. □

The subspace described in the proposition is, however, *not* a Dirac structure. This is due to the fact that the duality product $\langle\cdot,\cdot\rangle_M$ is *degenerate* in general, i.e. its value can be zero for nonzero discrete flows and/or efforts that lie in the kernel of $\mathbf{M}_p$, $\mathbf{M}_q$, or their transposes[28].

[27] A quadratic form is called *isotropic* if there exists a non-zero vector which is mapped to zero.

[28] Consider systems of conservation laws with $p=n$, $q=1$. In 1D, we have for Whitney finite elements on a simplicial triangulation or a polynomial approximation [42], $\dim\mathbf{e}^p = \dim\mathbf{f}^p + 1$ and $\dim\mathbf{e}^p = \dim\mathbf{f}^p + 1$, i.e. $\dim(\ker\mathbf{M}_p^T) = 1$ and $\dim(\ker\mathbf{M}_q^T) = 1$. On a 2D triangulation with Whitney forms, $\mathbf{M}_q$ will be square, while $\mathbf{M}_p$ will be fat, for a certain minimal grid size, i.e. $\ker\mathbf{M}_p \neq \emptyset$.

3.2.4 Discrete conservation laws

Instead of the mixed Galerkin approximation of (32) on the complete spatial domain Ω, we can approximate both conservation laws on the discrete, *oriented* geometric objects of dimension p and q (faces and edges in 2D, for example) of the discretization mesh. We obtain a *discrete representation* of the two conservation laws in the form

$$\begin{bmatrix} \mathbf{f}^p \\ \mathbf{f}^q \end{bmatrix} = \begin{bmatrix} \mathbf{0} & (-1)^r \mathbf{d}_p \\ \mathbf{d}_q & \mathbf{0} \end{bmatrix} \begin{bmatrix} \mathbf{e}^p \\ \mathbf{e}^q \end{bmatrix}. \tag{75}$$

$\mathbf{D}_p$ and $\mathbf{D}_q$ are considered *discrete derivative* matrices, which replace the exterior derivative in the original infinite-dimensional representation. If Whitney forms of lowest polynomial degree are used as finite element approximation bases, they represent the co-incidence or co-boundary relations between the discrete geometric objects associated to effort and flow forms. The term *co-incidence* matrix is preferred to *co-boundary* matrix in the PH framework to avoid confusion with the *system boundary*, see [55] or [61].

Replacing (75) in (55), we obtain the relations

$$\begin{aligned} (-1)^r \mathbf{M}_p \mathbf{d}_p + (\mathbf{K}_p + \mathbf{L}_p) = \mathbf{0} \\ \mathbf{M}_q \mathbf{d}_q + (\mathbf{K}_q + \mathbf{L}_q) = \mathbf{0} \end{aligned} \tag{76}$$

for the matrices of both representations.

4 Geometric discretization of the port-Hamiltonian system

By power-preserving projections of the discrete power variables (flows and efforts), we formulate an *approximate Dirac structure*, which is based on *non-degenerate* duality pairings between discrete bond variables. This Dirac structure admits different representations, in particular it can be written in an explicit input-output form. The consistent approximation of the constitutive relations, which defines a discrete Hamiltonian, finally yields the family of PH finite-dimensional state space models, which are parametrized by the power-preserving projections and the definitions of boundary control inputs.

4.1 Power-preserving projections and conjugated output maps

Due to the different approximation bases for flows and efforts, the matrices $\mathbf{M}_p$ and $\mathbf{M}_q$ can be non-square such that the duality products $\langle \mathbf{e}^p, \mathbf{M}_p \mathbf{f}^p \rangle$ and $\langle \mathbf{e}^q, \mathbf{M}_q \mathbf{f}^q \rangle$ are *degenerate*. An approximation Dirac structure must be based on a *non-degenerate* duality product between the variables of the discrete bond space. To this end, we will determine *power-preserving projections*

$$\tilde{\mathbf{e}}^p = \mathbf{P}_{ep} \mathbf{e}^p, \quad \tilde{\mathbf{e}}^q = \mathbf{P}_{eq} \mathbf{e}^q \qquad \text{and} \qquad \tilde{\mathbf{f}}^p = \mathbf{P}_{fp} \mathbf{f}^p, \quad \tilde{\mathbf{f}}^q = \mathbf{P}_{fq} \mathbf{f}^q. \tag{77}$$

such that

$$\tilde{N}_p := \dim \tilde{\mathbf{e}}^p = \dim \tilde{\mathbf{f}}^p \leq \operatorname{rank}(\mathbf{M}_p) \qquad \text{and} \qquad \tilde{N}_q := \dim \tilde{\mathbf{e}}^q = \dim \tilde{\mathbf{f}}^q \leq \operatorname{rank}(\mathbf{M}_q). \tag{78}$$

We refer to the vectors $\tilde{\mathbf{f}}^p, \tilde{\mathbf{e}}^p \in \mathbb{R}^{\tilde{N}_p}$, $\tilde{\mathbf{f}}^q, \tilde{\mathbf{e}}^q \in \mathbb{R}^{\tilde{N}_q}$ as *projected* discrete flows and efforts, as they can be interpreted as projections on subspaces of the original discrete bond spaces.

Example 3. In the 1D case, $p = q = 1$, using Whitney finite elements or the pseudo-spectral method [42], we have, $N = N_p = N_q$ and $M = M_p = M_q$ with $M = N + 1$. Fixing $\tilde{\mathbf{f}}^p = \mathbf{f}^p$, $\tilde{\mathbf{f}}^q = \mathbf{f}^q$ and $\mathbf{P}_{ep} = \mathbf{M}_p^T$, $\mathbf{P}_{eq} = \mathbf{M}_q^T$, the new efforts $\tilde{\mathbf{e}}^p$, $\tilde{\mathbf{e}}^q$ are projections of $\mathbf{e}^p$, $\mathbf{e}^q$ in direction of the kernel of $\mathbf{M}_p^T$ and $\mathbf{M}_q^T$, respectively.

The following definition summarizes the core property of power-preserving projections.

Definition 5. The discrete flow and effort projections (77) are *power-preserving* if they satisfy a discrete power balance

$$\langle \tilde{\mathbf{e}}^p, \tilde{\mathbf{f}}^p \rangle + \langle \tilde{\mathbf{e}}^q, \tilde{\mathbf{f}}^q \rangle + \langle \mathbf{e}^b, \mathbf{f}^b \rangle + \langle \hat{\mathbf{e}}^b, \hat{\mathbf{f}}^b \rangle = 0 \tag{79}$$

with the given boundary inputs $\mathbf{e}^b$, $\hat{\mathbf{e}}^b$ according to (64) and possibly modified boundary outputs

$$\mathbf{f}^b = \mathbf{S}_p^\mu \mathbf{e}^p, \qquad \hat{\mathbf{f}}^b = \hat{\mathbf{S}}_q^\nu \mathbf{e}^q. \tag{80}$$

Remark 6. If the projections satisfy $\mathbf{P}_{ep}^T \mathbf{P}_{fp} = \mathbf{M}_p$ and $\mathbf{P}_{eq}^T \mathbf{P}_{fq} = \mathbf{M}_q$, the "interior" part of the power balance (61) is exactly represented by the new flows and efforts, and (79) holds with the original, collocated outputs $\mathbf{f}_0^b$, $\hat{\mathbf{f}}_0^b$. If, however, $\tilde{N}_q < \text{rank}(\mathbf{M}_q)$ and/or $\tilde{N}_p < \text{rank}(\mathbf{M}_p)$, a part of the power, originally described by $\langle \mathbf{e}^p, \mathbf{M}_p \mathbf{f}^p \rangle + \langle \mathbf{e}^q, \mathbf{M}_q \mathbf{f}^q \rangle$, must be "swapped" to the boundary terms of (79) via the re-definition of the outputs. This way, the power-balance is maintained globally, and conservativeness of the finite-dimensional approximation is guaranteed.

To characterize the power-preserving projections and modified output maps that guarantee power continuity (79), we replace the definitions of projections, in- and outputs, and substitute $\mathbf{f}^p$, $\mathbf{f}^q$ according to the discrete representation (75) of the conservation laws. The new power variables are now expressed in terms of the original discrete efforts,

$$\underbrace{\begin{bmatrix} \tilde{\mathbf{f}}^p \\ \tilde{\mathbf{f}}^q \\ \hat{\mathbf{f}}^b \\ \mathbf{f}^b \end{bmatrix}}_{\bar{\mathbf{f}}} = \underbrace{\begin{bmatrix} \mathbf{0} & (-1)^r \mathbf{P}_{fp} \mathbf{d}_p \\ \mathbf{P}_{fq} \mathbf{d}_q & \mathbf{0} \\ \mathbf{0} & \hat{\mathbf{S}}_q \\ \mathbf{S}_p & \mathbf{0} \end{bmatrix}}_{\mathbf{E}^T} \underbrace{\begin{bmatrix} \mathbf{e}^p \\ \mathbf{e}^q \end{bmatrix}}_{\mathbf{e}}, \qquad \underbrace{\begin{bmatrix} \tilde{\mathbf{e}}^p \\ \tilde{\mathbf{e}}^q \\ \hat{\mathbf{e}}^b \\ \mathbf{e}^b \end{bmatrix}}_{\bar{\mathbf{e}}} = \underbrace{\begin{bmatrix} \mathbf{P}_{ep} & \mathbf{0} \\ \mathbf{0} & \mathbf{P}_{eq} \\ \hat{\mathbf{T}}_p & \mathbf{0} \\ \mathbf{0} & \mathbf{T}_q \end{bmatrix}}_{\mathbf{F}^T} \underbrace{\begin{bmatrix} \mathbf{e}^p \\ \mathbf{e}^q \end{bmatrix}}_{\mathbf{e}}. \tag{81}$$

Equation (79) must hold for arbitrary $\mathbf{e}^p$, $\mathbf{e}^q$, and we obtain the following matrix condition.

Proposition 6. *The effort and flow projections and output maps are* power-preserving*, if they satisfy the matrix equation*

$$(-1)^r \mathbf{d}_p^T \mathbf{P}_{fp}^T \mathbf{P}_{ep} + \mathbf{P}_{eq}^T \mathbf{P}_{fq} \mathbf{d}_q + \mathbf{T}_q^T \mathbf{S}_p + \hat{\mathbf{S}}_q^T \hat{\mathbf{T}}_p = \mathbf{0}. \tag{82}$$

The power-preserving projections and output maps are not unique. Different parametrization of the matrices, yield different finite-dimensional Dirac structures that approximate the original Stokes-Dirac structure of Proposition 1. Together with a consistent approximation of the constitutive equations, we can obtain PH approximate models with different numerical properties. A favorable parametrization will depend on the nature of the system (e.g. if the closure equations make the system hyperbolic or parabolic), the distribution and type of boundary inputs, and the application case.

In Section 5, we will illustrate the power-preserving projections at the example of Whitney approximation forms on a rectangular simplicial mesh in 2D. The degrees of freedom in the projections will allow for a trade-off between centered schemes and upwinding in the discretized PH models.

4.2 Dirac structure on the new bond space

The power-preserving projections and output maps that satisfy (82) define a *Dirac structure.* We verify that (81) is an *image* representations of this Dirac structure on the new discrete bond space. If the effort maps are invertible, an unconstrained input-output representation exists.

Proposition 7 (Image representation)**.** *Consider the discrete flow and effort vectors* $\bar{\mathbf{f}}$ *and* $\bar{\mathbf{e}}$ *as indicated in* (81)*.* $(\bar{\mathbf{f}}, \bar{\mathbf{e}})$ *is an element of the bond space* $\bar{\mathcal{F}} \times \bar{\mathcal{E}} = \mathbb{R}^{\tilde{N}_p + \tilde{N}_q + M_b + \hat{M}_b} \times \mathbb{R}^{\tilde{N}_p + \tilde{N}_q + M_b + \hat{M}_b}$*. Let* $\tilde{N}_p + \tilde{N}_q + \hat{M}_b + M_b = M_p + M_q$ *and the projection and output matrices satisfy the matrix condition* (82)*. If*

$$\text{rank}(\begin{bmatrix} \mathbf{P}_{ep} \\ \hat{\mathbf{T}}_p \end{bmatrix}) = M_p \qquad \textit{and} \qquad \text{rank}(\begin{bmatrix} \mathbf{P}_{eq} \\ \mathbf{T}_q \end{bmatrix}) = M_q, \tag{83}$$

then the subspace

$$\bar{\mathcal{D}} = \{ (\bar{\mathbf{f}}, \bar{\mathbf{e}}) \in \bar{\mathcal{F}} \times \bar{\mathcal{E}} \mid \bar{\mathbf{f}} = \mathbf{E}^T \mathbf{e}, \ \bar{\mathbf{e}} = \mathbf{F}^T \mathbf{e}, \ \mathbf{e} \in \mathbb{R}^{M^p + M^q} \}, \tag{84}$$

is a Dirac structure.

Proof. According to the definition of the image representation of a Dirac structure (see e.g. [59], Section 4.4.1) the dimensions of $\bar{\mathbf{f}}$ and $\bar{\mathbf{e}}$ must be less[29] or equal $\dim(\mathbf{e})$, which is ensured by $\tilde{N}_p+\tilde{N}_q+\hat{M}_b+M_b = M_p+M_q$. The condition $\operatorname{rank}([\mathbf{F}\ \ \mathbf{E}]) = M_p + M_q$ is satisfied by (83), from which $\operatorname{rank}(\mathbf{F}) = M_p + M_q$ follows. Moreover, the skew-symmetry condition $\mathbf{E}\mathbf{F}^T + \mathbf{F}\mathbf{E}^T = \mathbf{0}$ must hold. $\mathbf{E}\mathbf{F}^T + \mathbf{F}\mathbf{E}^T$ according to (81) gives

$$\begin{bmatrix} \mathbf{0} & \mathbf{d}_q^T\mathbf{P}_{fq}^T\mathbf{P}_{eq} + (-1)^r\mathbf{P}_{ep}^T\mathbf{P}_{fp}\mathbf{d}_p + \mathbf{S}_p^T\mathbf{T}_q + \hat{\mathbf{S}}_p^T\hat{\mathbf{T}}_q \\ (-1)^r\mathbf{d}_p^T\mathbf{P}_{fp}^T\mathbf{P}_{ep} + \mathbf{P}_{eq}^T\mathbf{P}_{fq}\mathbf{d}_q + \mathbf{T}_q^T\mathbf{S}_p + \hat{\mathbf{S}}_q^T\hat{\mathbf{T}}_p & \mathbf{0}, \end{bmatrix} \tag{85}$$

which equals zero by the characterization of power-preserving projections and output maps (82). ☐

Corollary 2 (Input-output representation)**.** *Under the conditions of Prop. 7, the Dirac structure admits an* unconstrainted input-output representation

$$\begin{aligned} \begin{bmatrix} -\tilde{\mathbf{f}}^p \\ -\tilde{\mathbf{f}}^q \end{bmatrix} &= \underbrace{\begin{bmatrix} \mathbf{0} & \mathbf{J}_p \\ \mathbf{J}_q & \mathbf{0} \end{bmatrix}}_{\mathbf{J}=-\mathbf{J}^T} \begin{bmatrix} \tilde{\mathbf{e}}^p \\ \tilde{\mathbf{e}}^q \end{bmatrix} + \underbrace{\begin{bmatrix} \mathbf{0} & \mathbf{B}_p \\ \mathbf{B}_q & \mathbf{0} \end{bmatrix}}_{\mathbf{B}} \begin{bmatrix} \hat{\mathbf{e}}^b \\ \mathbf{e}^b \end{bmatrix} \\ \begin{bmatrix} \hat{\mathbf{f}}^b \\ \mathbf{f}^b \end{bmatrix} &= \underbrace{\begin{bmatrix} \mathbf{0} & \mathbf{C}_q \\ \mathbf{C}_p & \mathbf{0} \end{bmatrix}}_{\mathbf{C}=\mathbf{B}^T} \begin{bmatrix} \tilde{\mathbf{e}}^p \\ \tilde{\mathbf{e}}^q \end{bmatrix} + \underbrace{\begin{bmatrix} \mathbf{0} & \mathbf{D}_q \\ \mathbf{D}_p & \mathbf{0} \end{bmatrix}}_{\mathbf{D}=-\mathbf{D}^T} \begin{bmatrix} \hat{\mathbf{e}}^b \\ \mathbf{e}^b \end{bmatrix}. \end{aligned} \tag{86}$$

with

$$\mathbf{J}_p = -\mathbf{J}_q^T, \quad \mathbf{B}_p = \mathbf{C}_p^T,\ \mathbf{B}_q = \mathbf{C}_q^T, \quad \mathbf{D}_q = \mathbf{D}_p^T. \tag{87}$$

Proof. The (skew-)symmetry conditions can be summarized as

$$\begin{bmatrix} -\mathbf{J}_p & -\mathbf{B}_p \\ \mathbf{C}_q & \mathbf{D}_q \end{bmatrix} + \begin{bmatrix} -\mathbf{J}_q & -\mathbf{B}_q \\ \mathbf{C}_p & \mathbf{D}_p \end{bmatrix}^T = \begin{bmatrix} \mathbf{0} & \mathbf{0} \\ \mathbf{0} & \mathbf{0} \end{bmatrix}. \tag{88}$$

By invertibility of the matrices in (83),

$$\begin{bmatrix} -\mathbf{J}_p & -\mathbf{B}_p \\ \mathbf{C}_q & \mathbf{D}_q \end{bmatrix} = \begin{bmatrix} (-1)^r\mathbf{P}_{fp}\mathbf{d}_p \\ \hat{\mathbf{S}}_q \end{bmatrix} \begin{bmatrix} \mathbf{P}_{eq} \\ \mathbf{T}_q \end{bmatrix}^{-1}, \quad \begin{bmatrix} -\mathbf{J}_q & -\mathbf{B}_q \\ \mathbf{C}_p & \mathbf{D}_p \end{bmatrix} = \begin{bmatrix} \mathbf{P}_{fq}\mathbf{d}_q \\ \mathbf{S}_p \end{bmatrix} \begin{bmatrix} \mathbf{P}_{ep} \\ \hat{\mathbf{T}}_p \end{bmatrix}^{-1}. \tag{89}$$

Substituting these relations in (88) and multiplying with $\begin{bmatrix} \mathbf{P}_{ep}^T & \hat{\mathbf{T}}_p^T \end{bmatrix}$ from the left and $\begin{bmatrix} \mathbf{P}_{eq} \\ \mathbf{T}_q \end{bmatrix}$ from the right, yields the left hand side of (82). The right hand side being zero, this proves (skew-)symmetry of the matrices (87) of the input-output representation. ☐

The proposition is a generalization of Prop. 20 in [42] for the 1D case and the pseudo-spectral method. Note that the rank condition (83) on the effort and flow and boundary maps is sufficient (not necessary) for the subspace (84) to be a Dirac structure. The fact that both matrices in (83) are assumed square and invertible, guarantees the input-output representation in the corollary.

4.3 Finite-dimensional port-Hamiltonian model

To render the input-output representation of the Dirac structure a finite-dimensional port-Hamiltonian model of a *canonical system of two conservation laws*, we replace the projected discrete flow variables by time derivatives of *discrete states*[30]

$$-\tilde{\mathbf{f}}^p =: \dot{\mathbf{p}} \in \mathbb{R}^{\tilde{N}_p}, \qquad -\tilde{\mathbf{f}}^q =: \dot{\mathbf{q}} \in \mathbb{R}^{\tilde{N}_q}. \tag{90}$$

[29] This is the case of a *relaxed* image representation.

[30] If a flow variable is defined differently, as in the case of the 2D SWE with the additional rotation term, this has to be accounted for also in the discrete equation.

On the other hand, the projected efforts need to be replaced by the partial derivatives of a suitable discrete Hamiltonian $\tilde{H}_d(\tilde{\mathbf{p}}, \tilde{\mathbf{q}})$

$$\tilde{\mathbf{e}}^p = \left(\frac{\partial \tilde{H}_d}{\partial \tilde{\mathbf{p}}}\right)^T \in \mathbb{R}^{\tilde{N}_p}, \qquad \tilde{\mathbf{e}}^q = \left(\frac{\partial \tilde{H}_d}{\partial \tilde{\mathbf{q}}}\right)^T \in \mathbb{R}^{\tilde{N}_q}. \tag{91}$$

The discrete Hamiltonian must be defined in such a way that the discrete effort variables represent a *consistent* approximation of their continuous counterpart. We present the discretization of the constitutive equations in detail in the FE example of Section 5.

With the state, input and output vectors

$$\mathbf{x} = \begin{bmatrix} \tilde{\mathbf{p}} \\ \tilde{\mathbf{q}} \end{bmatrix}, \quad \mathbf{u} = \begin{bmatrix} \hat{\mathbf{e}}^b \\ \mathbf{e}^b \end{bmatrix}, \quad \mathbf{y} = \begin{bmatrix} \hat{\mathbf{f}}^b \\ \mathbf{f}^b \end{bmatrix}, \tag{92}$$

the resulting state space model

$$\begin{aligned} \dot{\mathbf{x}} &= \mathbf{J}\nabla H_d(\mathbf{x}) + \mathbf{B}\mathbf{u} \\ \mathbf{y} &= \mathbf{B}^T\nabla H_d(\mathbf{x}) + \mathbf{D}\mathbf{u} \end{aligned} \tag{93}$$

has PH form and the discrete energy satisfies the balance equation

$$\dot{H}_d = -\mathbf{y}^T\mathbf{u}, \tag{94}$$

which is the finite-dimensional counterpart of (7). The PH form allows to easily interconnect the finite-dimensional model of the system of two conservation laws with other subsystems in a power-preserving way, which is the basis for energy-based control design *by interconnection* see e.g. [40].

Can we use the projections to define new approximation bases that can be used in the variational problem and directly yield square and invertible matrices $\mathbf{M}_p$, $\mathbf{M}_q$?

5 Example: Whitney forms on a 2D rectangular grid

To illustrate the steps to obtain an approximate PH state space model with desired boundary inputs by *geometric discretization*, we consider a 2-dimensional rectangular domain $\Omega = (0, L_x) \times (0, L_y) \subset \mathbb{R}^2$, with boundary $\partial\Omega$, covered by a regular, *oriented* simplicial triangulation $\mathcal{T}_h$, as sketched in Fig. 2. The approximation bases for flows and efforts (39), (40) are composed of *Whitney forms* [66] of lowest polynomial degree, which can be constructed based on the *barycentric* node weights [14]. The degrees of freedom are directly associated to the *nodes*, directed *edges* and *faces* of the mesh. The well-known geometric discretization of Maxwell's equations [12] is based on Whitney forms, and the resulting finite-dimensional models feature the (co-)incidence matrices of the underlying discretization meshes [10]. They can be considered a *direct representation* of the physical laws on the discrete balance regions of the triangulation, which underscores the strong relation to *Tonti's cell method* [57]. In contrast to [10], [57], where the conservation laws are evaluated on *dual* or *staggered* grids, we start with a *single* mesh. Nevertheless, in our approach, the projections of the original degrees of freedom gives rise to interpret the projected flows and efforts in terms of *topological duality.*

5.1 Mesh, matrices and dimensions

Using Whitney basis forms, the degrees of freedom in the mixed Galerkin approach are associated to integrals of distributed quantities on the k-simplices of the mesh. The dimensions of the (initial) discrete flow and effort vectors equal the numbers of corresponding nodes, edges and faces on the grid. The same holds for the discrete efforts on the boundary, which are designated inputs and are localized at the corresponding boundary nodes and edges, see Table 1.

The mixed Galerkin approximation of the Stokes-Dirac structure yields a set of matrices with different sizes and ranks, see Table 2. The construction of power-preserving projections and conjugated output matrices that satisfy the matrix equation (82), is based on rank considerations of the involved matrix products.

Table 1: Dimensions of discrete flow and efforts spaces on the rectangular $N \times M$ simplicial grid.

Vector(s)	$\mathbf{f}^p$	$\mathbf{f}^q$, $\mathbf{e}^q$	$\mathbf{e}^p$	$\mathbf{e}^p_b$, $\mathbf{e}^q_b$
Dimension	$2NM$	$3NM{+}N{+}M$	$(N{+}1)(M{+}1)$	$2(N{+}M)$
Symbol(s)	N_p	$N_q = M_q$	M_p	M_p^b, M_q^b

Table 2: Sizes and ranks of the matrices for the discrete variational problem and the direct discret model, respectively. $N, M > 2$.

Matrix	$\mathbf{M}_p$	$\mathbf{K}_p + \mathbf{L}_p$	$\mathbf{d}_p$	$\mathbf{M}_q$	$\mathbf{K}_q + \mathbf{L}_q$	$\mathbf{d}_q$	$\mathbf{L}_p = \mathbf{L}_q^T$
Size	$M_p \times N_p$	$M_p \times N_q$	$N_p \times N_q$	$N_q \times N_q$	$N_q \times M_p$	$N_q \times M_p$	$M_p \times N_q$
Rank	$M_p - 2$	$M_p - 2$	N_p	$2(M_p - 2)$	$M_p - 1$	$M_p - 1$	$2(M + N) - 1$

5.2 Power-preserving projections, in- and outputs

We describe the different matrices that define the discrete power variables on the projected bond space.

5.2.1 Input trace matrices and effort projections

Identifying the elements of the input vector $\mathbf{u} = \begin{bmatrix}(\hat{\mathbf{e}}^b)^T & (\mathbf{e}^b)^T\end{bmatrix}^T$ with effort degrees of freedom on the boundary nodes and edges corresponds to a consistent imposition of the effort boundary conditions in the finite-dimensional model. To arrive at the input-output representation (86), the matrices

$$\mathbf{\Pi}_p := \begin{bmatrix}\mathbf{P}_{ep} \\ \hat{\mathbf{T}}_p\end{bmatrix} \quad \text{and} \quad \mathbf{\Pi}_q := \begin{bmatrix}\mathbf{P}_{eq} \\ \mathbf{T}_q\end{bmatrix} \tag{95}$$

should be square and invertible. Choosing $\mathbf{\Pi}_p$ and $\mathbf{\Pi}_q$ as *permutation matrices*, each projected effort/boundary effort is assigned to an interior/boundary simplex. The property $\mathbf{\Pi}_{p/q}^{-1} = \mathbf{\Pi}_{p/q}^T$ makes the matrices of the state space model, which result from a right multiplication with $\mathbf{\Pi}_{p/q}^{-1}$, particularly simple.

5.2.2 Flow/state projections

For the considered rectangular simplicial grid, we propose the following constructions for $\mathbf{P}_{fp}$ and $\mathbf{P}_{fq}$. We omit the derivations, and illustrate the results graphically.

Each element $\tilde{f}_i^p$, $i = 1, \ldots, \tilde{N}_p$, of $\tilde{\mathbf{f}}^p = \mathbf{P}_{fp}\tilde{\mathbf{p}}$ is related to a 2-chain (a weighted formal sum of 2-simplices), located around the node associated to $\tilde{e}_i^p$. The node and the weighted 2-chain can be considered, hence, *topologically dual* objects. The weights of the 2-simplices around a node, are illustrated in Fig. 3. The index *I* refers to the lower right, *II* to the upper left triangles and $\alpha_\nu + \beta_\nu + \gamma_\nu = 1$,

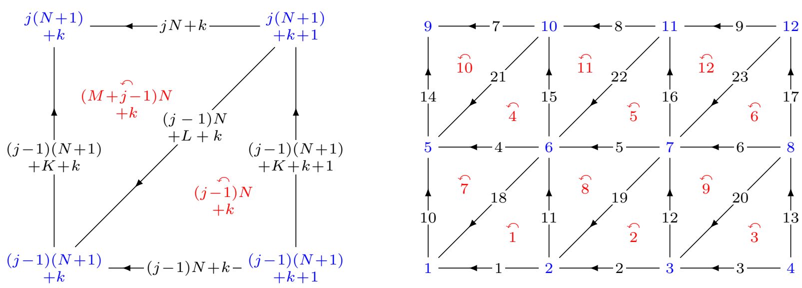

Figure 2: Left: Numbering of nodes, edges and faces on a $N \times M$ rectangular simplicial mesh. $K = (M+1)N$, $L = K + M(N+1)$. Right: 3×2 mesh.

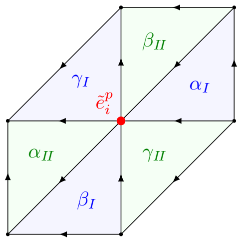

Figure 3: Illustration of an element of the row elements of $\mathbf{P}_{fp}$, associated to a discrete flow variable $\tilde{f}_i^p$. Defined as a weighted sum of original discrete flows on the neighboring 2-simplices, it can be considered also topologically dual to $\tilde{e}_i^p$.

$\nu \in \{I, II\}$ holds[31]. This convex combination of weights ensures that

$$\sum_{i=1}^{\tilde{N}_p} \tilde{p}_i = \sum_{j=1}^{N_p} p_j - \epsilon_p, \tag{96}$$

where ϵ_p is a weighted sum of the original discrete states p_j on 2-simplices around boundary input nodes. ϵ_p describes a defect of the total conserved quantity on the original grid. This defect at the boundary must be considered in the consistent definition of the discrete constitutive equations as shown further below.

Remark 7. By the topological duality between the elements of $\tilde{\mathbf{f}}^p$ and $\tilde{\mathbf{e}}^p$ as illustrated in Fig. 3, it is easy to imagine that the deviation ϵ^p can be related to well-known effects from the discretization with staggered grids, like ghost values, see e.g. [38] for a discussion from the PH point of view.

A related interpretation holds for the different elements of the projected flow vector $\tilde{\mathbf{f}}^q = \mathbf{P}_{fq}\mathbf{f}^q$. As shown in Fig. 4, each element of $\tilde{\mathbf{f}}^q$ can be considered dual to a discrete effort $\tilde{e}_i^q$ on a horizontal, vertical or diagonal edge (drawn in red). $\tilde{f}_i^p$ is constructed as a linear combination of the elements of $\tilde{\mathbf{f}}^q$ on adjacent edges. The weights can be clustered, which corresponds to a decomposition of $\tilde{f}_i^q$ into a rotational part and components along and across the effort edge. Only the latter part (drawn in blue) contributes to the discrete constitutive equations as discussed further below.

5.2.3 Conjugated discrete outputs

Like the projected flows and efforts, the discrete outputs $\mathbf{f}^b = \mathbf{S}_p\mathbf{e}^p$ and $\hat{\mathbf{f}}^b = \hat{\mathbf{S}}_q\mathbf{e}^q$ are constructed as weighted sums of the discrete efforts in the vicinity of the dual boundary input, see Fig. 5. f_i^b is defined by a convex sum of node efforts. Note that $\hat{f}_i^b$ is composed of a "rotation" part and a convex sum associated to the direct neighbor edges.

Remark 8. By reconstructing the rotational components of $\tilde{\mathbf{q}}$ from the given quantities, can be used to discretize the vorticity term in the shallow water equation (14).

Show by short calculation that the models indeed have no feedthrough.

5.3 Discrete constitutive equations

To obtain a consistent numerical approximation of the system of conservation laws, the discrete states $\tilde{\mathbf{p}}$, $\tilde{\mathbf{q}}$ and the above-defined efforts $\tilde{\mathbf{e}}^p$, $\tilde{\mathbf{e}}^q$ must be related via discrete constitutive relations that are consistent with the continuous ones. We consider the case of linear constitutive equations

$$e_p = \delta_p H = *p, \qquad e_q = \delta_q H = - * q. \tag{97}$$

[31]The weights can be different from node to node. For simplicity, we fix the same pairs (α_I, β_I) and $(\alpha_{II}, \beta_{II})$ on the whole mesh.

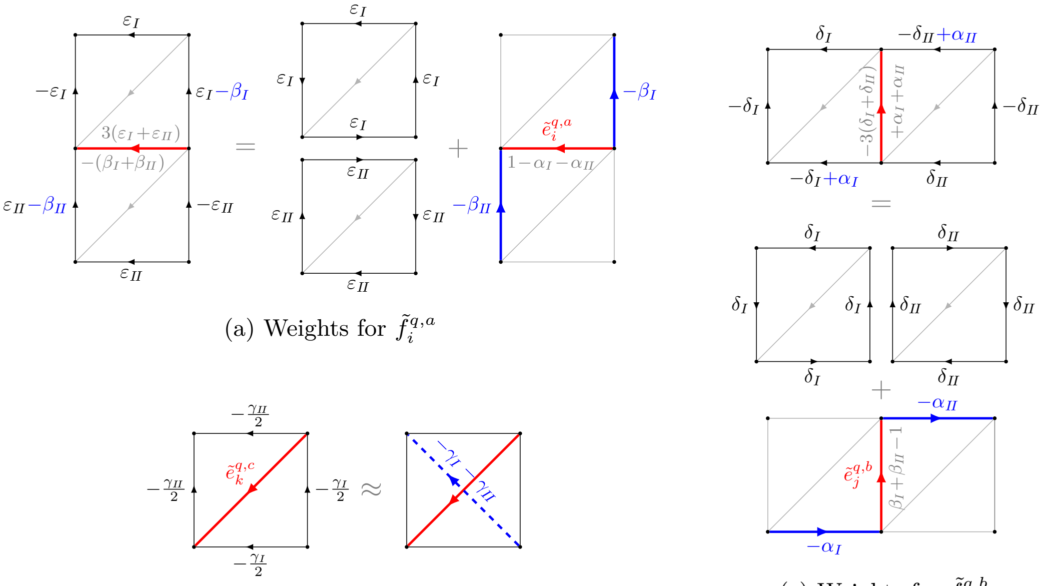

(a) Weights for $\tilde{f}_i^{q,a}$

(b) Weights for $\tilde{f}_i^{q,c}$

(c) Weights for $\tilde{f}_i^{q,b}$

Figure 4: Weights on directed edges to define the elements of $\tilde{\mathbf{f}}^q$ which are dual to $\tilde{\mathbf{e}}^q$. (a), (b) and (c) show the construction based on discrete efforts in horizontal, diagonal and vertical direction (red). The blue edges and weights display the contributions to the discrete constitutive equation, which is a flux *across* the effort edge. $\delta_{I/II} = \frac{1}{8} + \frac{1}{4}(\alpha_{I/II} - \beta_{I/II})$, $\varepsilon_{I/II} = \frac{1}{8} - \frac{1}{4}(\alpha_{I/II} - \beta_{I/II})$.

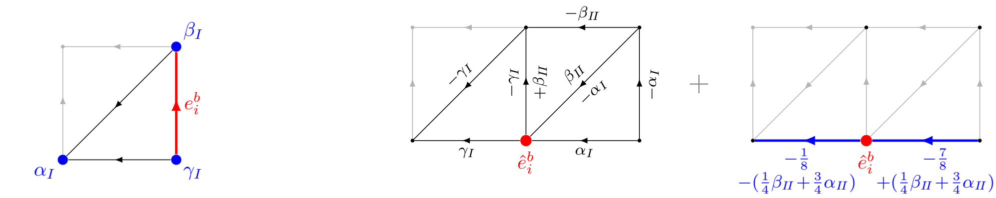

(a) Illustration of an element f_i^b.

(b) Illustration an element $\hat{f}_i^b$.

Figure 5: Illustration of the elements of the output vectors $\mathbf{f}^b = \mathbf{S}_p \mathbf{e}^p$ and $\hat{\mathbf{f}}^b = \hat{\mathbf{S}}_q \mathbf{e}^q$ as a weighted sum of node/edge efforts in the neighborhood of the input edge/node.

that are derived from the simple quadratic Hamiltonian

$$H = \int_\Omega (\frac{1}{2} p \wedge *p + \frac{1}{2} q \wedge *q). \tag{98}$$

The discrete constitutive equations will be expressed by

$$\tilde{\mathbf{e}}^p = \mathbf{Q}_p \tilde{\mathbf{p}}, \qquad \tilde{\mathbf{e}}^q = \mathbf{Q}_q \tilde{\mathbf{q}} \tag{99}$$

with positive definite, diagonal matrices $\mathbf{Q}_p$, $\mathbf{Q}_q$. $\tilde{\mathbf{p}}$ and $\tilde{\mathbf{q}}$ are constructed as linear combinations of integral conserved quantities on the 2- and 1-simplices of the discretization grid. By the construction illustrated above, we can think $\tilde{\mathbf{p}}$, $\tilde{\mathbf{q}}$ localized on a (virtual) *dual* grid, whose localization is parameterized by the projection parameters $\alpha_{I/II}$ and $\beta_{I/II}$. This justifies the interpretation of $\mathbf{Q}_p$, $\mathbf{Q}_q$ as (diagonal) *discrete Hodge matrices* that replace the Hodge star in (97).

For the consistent construction of these Hodge matrices, we assume a steady state. In this case, the elements of $\tilde{\mathbf{e}}^p$ must represent "average" values of p on the weighted balance areas[32] for the $\tilde{p}_i$. Accordingly, the elements of $\tilde{\mathbf{e}}^q$ must reflect the integral flux of the vector field[33] $q^\sharp$ across the corresponding horizontal,

[32]Precisely, the average value of the coefficient function of the 2-form p.
[33]Index raising of the 1-form q.

vertical or diagonal edges. The weights in the definition of $\tilde{q}_i$ that belong to edges perpendicular to the $\tilde{e}_i^q$ determine the diagonal elements of $\mathbf{Q}_q^{-1}$.

5.4 Simulation study

We consider the linear wave equation with Hamiltonian density (98) on a square domain $\Omega = [0, 20]\times[0, 20]$ to illustrate the effects of different projection parameters, see Table 3. We impose the boundary conditions

$$e^p(0,0) = u(t) = \begin{cases} \sin^2(\frac{\pi}{8}t), & 0 \leq t < 8 \\ 0 & t \geq 8 \end{cases}, \qquad e^q(x,y) = 0 \quad \text{on} \quad \partial\Omega. \tag{100}$$

by the input trace matrices

$$\hat{\mathbf{T}}_p = \begin{bmatrix} 1 & 0 & \dots & 0 \end{bmatrix}, \qquad \mathbf{T}_q = \mathbb{I}_b^1, \tag{101}$$

where $\mathbb{I}_b^1 \in \mathbb{R}^{M_b \times N_q}$ is the matrix composed of unit row vectors associated to boundary edges, and the inputs to the simulation model

$$\hat{e}^b(t) = u(t), \quad \mathbf{e}^b(t) = \mathbf{0}. \tag{102}$$

Table 3: Parameter sets for the simulation.

	α_I	α_{II}	β_I	β_{II}
Parameters 1	1/2	1/3	1/3	1/2
Parameters 2	1/2	1/4	1/4	1/2
Parameters 3	2/3	1/6	1/6	2/3
Parameters 4	7/8	1/32	1/32	7/8

Fig. 6 shows the simulated propagation of the wave in radial direction under different parametrizations of the method, see Table 3. The red line displays a circle with radius $t_{sim} - T/2 = 16$, as a reference for the maximum of the wavefront[34]. The first parameter set produces a *centered* numerical scheme with respect to the propagation direction. The three remaining parameter sets correspond to a stronger weighting of the simplices in the propagation direction for the computation of $\tilde{f}_i^p$, see Fig. 3. As a result, the numerical schemes can be considered different realizations of "upwinding". Observe also the different variation from the shape of a quarter circle, which are due to the non-isotropic mesh and the different weights $\alpha_{I/II}$, $\beta_{I/II}$.

5.5 Spectral approximation

For a short analysis of the spectral approximation properties, we consider the 1D wave equation on a domain $\Omega = [0, 1]$, which is characterized by the degree $p = 1$ (instead of $p = 2$) of the first conserved quantity differential form. With the quadratic Hamiltonian as in (98), the sign of the second constitutive equation $e^q = *q$ changes. The exponent in the canonical differential operator now becomes $r = pq+1 = 2$. Table 4 shows the approximation of the spectrum of the canonical differential operator of the Stokes-Dirac structure (exact eigenvalues $\pm\frac{2k-1}{2}\pi i$, $k = 1, 2, 3, \dots$) under homogeneous Dirichlet boundary conditions. As the eigenvalues remain purely imaginary, only the magnitude of the imaginary part is indicated. From $\alpha = 0$ to $\alpha = 0.5$, the error for low frequencies decreases, while it increases for high frequencies. All frequencies are under-estimated with respect to the exact values. For $\alpha = 0.5$, every two eigenvalue pairs coincide at values that approximate the original spectrum best. This centered parameter choice is certainly more appropriate for a diffusive system. We will therefore, in a next step, analyze the spectral approximation of the Dirac structure for the parabolic case of constitutive equations and boundary conditions from the heat equation.

[34]Note that the plots in Fig. 6 represent the discrete, projected efforts $\tilde{e}_i^p$ *in the nodes* of the mesh. An appropriate localization of the values of $\tilde{\mathbf{p}}$ would be the *weighted* barycenters of the areas according to Fig. 3. This would advance the plotted wavefront in the propagation direction.

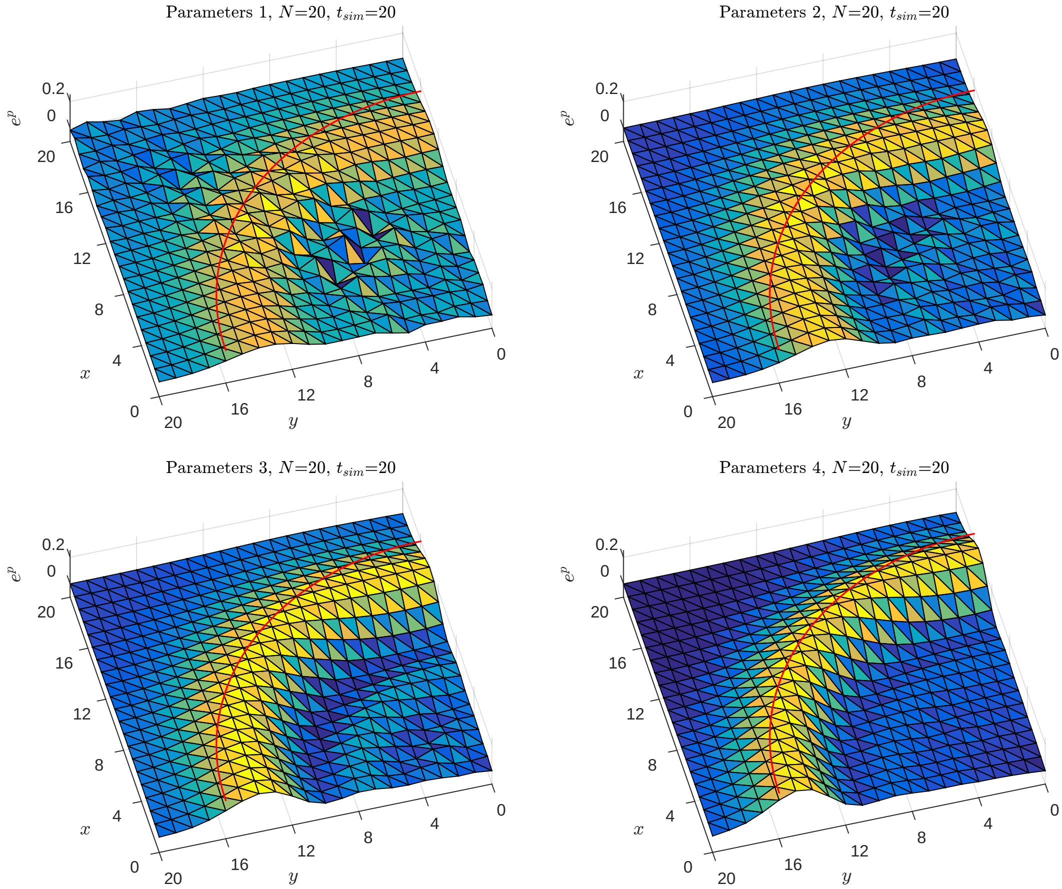

Figure 6: Propagation of a wave due to point-wise boundary excitation under different parametrizations of the method. Snapshots at $t_{sim} = 16$.

6 Conclusions

We introduced the weak form of the Stokes-Dirac structure with boundary inputs of different causality. This Stokes-Dirac structure is the underlying geometric structure to represent power continuity in a port-Hamiltonian distributed-parameter system. At the example of a system of two conservation laws with canonical interdomain coupling, we described the mixed Galerkin discretization of the Stokes-Dirac structure in a general way. To obtain finite-dimensional approximate models in port-Hamiltonian form with the prescribed boundary inputs – as basis for the interconnection of multi-physics models, control design and simulation – we proposed power-preserving projections. These maps on the space of discrete bond variables (the mixed Galerkin degrees of freedom associated with flows and efforts) allow to define non-degenerate duality pairings on a new bond spaces, leading to finite-dimensional approximate Dirac structures. The latter admit several representations, one of them the input-output-representation. Port-Hamiltonian state space models are obtained, if in addition, the energy and the constitutive equations are approximated consistently. At the example of Whitney finite elements we demonstrated the discretization procedure and gave interpretations of the resulting discretization schemes.

The proposed method is, to the best of our knowledge, the first method which allows for a structure-preserving discretization of port-Hamiltonian distributed-parameter systems in more than one spatial dimension with a systematic treatment of different boundary inputs and the possibility to tune the discretized models between centered schemes and upwinding. The proposed family of approximation Dirac structures avoids a direct feedthrough in the state space model and the over-estimation of higher frequencies in the approximate spectrum, which is the case for the method presented in [29], where the efforts instead of the flow degrees of freedom are projected. The weak form of the Stokes-Dirac structure is

Table 4: Values of the imaginary parts for the discretized wave equation with different projection parameters, compared to the exact values. Grid size $N = 20$.

k	Exact	$\alpha = 0$	$\alpha = 0.1$	$\alpha = 0.2$	$\alpha = 0.3$	$\alpha = 0.4$	$\alpha = 0.5$
1	1.5708	1.5321	1.5392	1.5464	1.5539	1.5614	1.5692
2	4.7124	4.5873	4.5985	4.6122	4.6284	4.6473	1.5692
3	7.8540	7.6156	7.6013	7.5974	7.6045	7.6231	4.6689
4	10.9956	10.5993	10.5115	10.4509	10.4193	8.4371	4.6689
5	14.1372	13.5207	13.2958	13.1256	13.0148	9.6285	7.6537
10	29.8451	26.6130	24.4593	22.6179	17.4897	15.0650	12.9890
20	61.2611	39.8826	31.9591	24.9858	21.8185	20.4059	19.9383

the key feature that allows to include additional effects such as dissipation or diffusion or, more generally, to tackle the discretization of port-Hamiltonian systems with general and higher order interconnection operators and distributed inputs.

Current and future work concerns the application of the method to the port-Hamiltonian representation of the heat equation, which shares the same Stokes-Dirac structure, the analysis of system-theoretic properties of the discretized models in view of control design and the interface to existing finite-element and simulation software. Moreover, we intend to include the discretization of the nonlinear constitutive relations for the 2D shallow water equations in our *open* models and clarify the links with recent work on geometric mixed finite elements like [19], [20], where in- and outputs are not explicitly taken into account, and upwinding in differential forms as presented in [18].

References

[1] Ralph Abraham, Jerrold E Marsden, and Tudor Ratiu. *Manifolds, tensor analysis, and applications*, volume 75. Springer Science & Business Media, 2012.

[2] R Altmann and P Schulze. A port-hamiltonian formulation of the navier–stokes equations for reactive flows. *Systems & Control Letters*, 100:51–55, 2017.

[3] Robert Altmann and Philipp Schulze. On the port-hamiltonian structure of the navier-stokes equations for reactive flows. *Technical Report, TU Berlin*, 2016.

[4] Akio Arakawa and Vivian R Lamb. A potential enstrophy and energy conserving scheme for the shallow water equations. *Monthly Weather Review*, 109(1):18–36, 1981.

[5] Douglas Arnold, Richard Falk, and Ragnar Winther. Finite element exterior calculus: from hodge theory to numerical stability. *Bulletin of the American mathematical society*, 47(2):281–354, 2010.

[6] Vladimir Igorevich Arnold. *Mathematical methods of classical mechanics*, volume 60. Springer Science & Business Media, 1989.

[7] A Baaiu, F Couenne, L Lefevre, Y Le Gorrec, and M Tayakout. Structure-preserving infinite dimensional model reduction: Application to adsorption processes. *Journal of Process Control*, 19(3):394–404, 2009.

[8] R Byron Bird, Warren E Stewart, and Edwin N Lightfoot. *Transport phenomena*. John Wiley & Sons, 2002.

[9] Pavel B Bochev and James M Hyman. Principles of mimetic discretizations of differential operators. In *Compatible spatial discretizations*, pages 89–119. Springer, 2006.

[10] A Bossavit and L Kettunen. Yee-like schemes on a tetrahedral mesh, with diagonal lumping. *International Journal of Numerical Modelling Electronic Networks Devices and Fields*, 12:129–142, 1999.

[11] Alain Bossavit. Differential forms and the computation of fields and forces in electromagnetism. *Eur. J. Mech. B*, 10(5):474–488, 1991.

[12] Alain Bossavit. *Computational electromagnetism: variational formulations, complementarity, edge elements.* Academic Press, 1998.

[13] Alain Bossavit. How weak is the" weak solution" in finite element methods? *IEEE transactions on magnetics*, 34(5):2429–2432, 1998.

[14] Alain Bossavit. Generating whitney forms of polynomial degree one and higher. *IEEE transactions on magnetics*, 38(2):341–344, 2002.

[15] Susanne Brenner and Ridgway Scott. *The mathematical theory of finite element methods*, volume 15. Springer Science & Business Media, 2008.

[16] Haim Brezis. *Functional analysis, Sobolev spaces and partial differential equations.* Springer Science & Business Media, 2011.

[17] Flávio Luiz Cardoso-Ribeiro, Denis Matignon, and Valérie Pommier-Budinger. A port-Hamiltonian model of liquid sloshing in moving containers and application to a fluid-structure system. *Journal of Fluids and Structures*, 69:402–427, 2017.

[18] S. H. Christiansen. Upwinding in finite element systems of differential forms. In *Foundations of computational mathematics, Budapest 2011*, volume 403 of *London Math. Soc. Lecture Note Ser.* Cambridge Univ. Press, 2013.

[19] CJ Cotter and Jemma Shipton. Mixed finite elements for numerical weather prediction. *Journal of Computational Physics*, 231(21):7076–7091, 2012.

[20] Colin J Cotter and John Thuburn. A finite element exterior calculus framework for the rotating shallow-water equations. *Journal of Computational Physics*, 257:1506–1526, 2014.

[21] Ruth F Curtain and Hans Zwart. An introduction to infinite-dimensional linear systems theory. 1995.

[22] Mathieu Desbrun, Eva Kanso, and Yiying Tong. Discrete differential forms for computational modeling. In *Discrete differential geometry*, pages 287–324. Springer, 2008.

[23] Vincent Duindam, Alessandro Macchelli, Stefano Stramigioli, and Herman Bruyninckx. *Modeling and Control of Complex Physical Systems: The Port-Hamiltonian Approach.* Springer Science & Business Media, 2009.

[24] Hector O Fattorini. Boundary control systems. *SIAM Journal on Control*, 6(3):349–385, 1968.

[25] Enrique D Fernandez-Nieto, Joel Marin, and Jerome Monnier. Coupling superposed 1d and 2d shallow-water models: Source terms in finite volume schemes. *Computers & Fluids*, 39(6):1070–1082, 2010.

[26] Harley Flanders. *Differential Forms with Applications to the Physical Sciences*, volume 197. Academic Press New York, 1963.

[27] Claude Gasquet and Patrick Witomski. *Fourier analysis and applications: filtering, numerical computation, wavelets*, volume 30. Springer Science & Business Media, 1999.

[28] C. Geuzaine. GetDP: a general finite-element solver for the de Rham complex. In *PAMM Volume 7 Issue 1. Special Issue: Sixth International Congress on Industrial Applied Mathematics (ICIAM07) and GAMM Annual Meeting, Zürich 2007*, volume 7, pages 1010603–1010604. Wiley, 2008.

[29] G. Golo, V. Talasila, A. van der Schaft, and B. Maschke. Hamiltonian discretization of boundary control systems. *Automatica*, 40(5):757–771, May 2004.

[30] G. Golo, V. Talasila, and A.J. van der Schaft. Approximation of the telegrapher's equations. In *Decision and Control, 2002, Proceedings of the 41st IEEE Conference on*, volume 4, pages 4587–4592 vol.4, Dec 2002.

[31] F. Hecht. New development in freefem++. *J. Numer. Math.*, 20(3-4):251–265, 2012.

[32] Jan S Hesthaven and Tim Warburton. *Nodal discontinuous Galerkin methods: algorithms, analysis, and applications*. Springer Science & Business Media, 2007.

[33] RR Hiemstra, D Toshniwal, RHM Huijsmans, and Marc I Gerritsma. High order geometric methods with exact conservation properties. *Journal of Computational Physics*, 257:1444–1471, 2014.

[34] Darryl D Holm. *Geometric mechanics: Dynamics and symmetry*. Imperial College Press, 2011.

[35] Birgit Jacob and Hans Zwart. *Linear port-Hamiltonian systems on infinite-dimensional spaces*, volume 223. Springer Science & Business Media, 2012.

[36] Tosio Kato. *Perturbation theory for linear operators*, volume 132. Springer, 1995.

[37] P. Kotyczka. Finite volume structure-preserving discretization of 1D distributed-parameter port-Hamiltonian systems. In *2nd IFAC Workshop on Control of Systems Governed by Partial Differential Equations, Bertinoro, Italy*, volume 49, pages 298–303. Elsevier, 2016.

[38] P. Kotyczka and B. Maschke. Discrete port-Hamiltonian formulation and numerical approximation for systems of two conservation laws. *at - Automatisierungstechnik*, 2017.

[39] Yann Le Gorrec, Hans Zwart, and Bernhard Maschke. Dirac structures and boundary control systems associated with skew-symmetric differential operators. *SIAM Journal on Control and Optimization*, 44(5):1864–1892, 2005.

[40] A. Macchelli. Energy shaping of distributed parameter port-hamiltonian systems based on finite element approximation. *Syst. Control Lett.*, 60:579–589, 2011.

[41] Jerrold E Marsden, George W Patrick, and Steve Shkoller. Multisymplectic geometry, variational integrators, and nonlinear pdes. *Communications in Mathematical Physics*, 199(2):351–395, 1998.

[42] R Moulla, L Lefévre, and Bernhard Maschke. Pseudo-spectral methods for the spatial symplectic reduction of open systems of conservation laws. *Journal of Computational Physics*, 231(4):1272–1292, 2012.

[43] Gou Nishida, Bernhard Maschke, and Ryojun Ikeura. Boundary integrability of multiple stokes–dirac structures. *SIAM Journal on Control and Optimization*, 53(2):800–815, 2015.

[44] Suhas Patankar. *Numerical heat transfer and fluid flow*. CRC press, 1980.

[45] Henry M Paynter. *Analysis and design of engineering systems*. MIT press, 1961.

[46] Mónika Polner and JJW van der Vegt. A hamiltonian vorticity–dilatation formulation of the compressible euler equations. *Nonlinear analysis: theory, methods & applications*, 109:113–135, 2014.

[47] Alfio Quarteroni and Alberto Valli. *Numerical Approximation of Partial Differential Equations*. Springer, 1994.

[48] Hector Ramirez, Bernhard Maschke, and Daniel Sbarbaro. Irreversible port-hamiltonian systems: A general formulation of irreversible processes with application to the cstr. *Chemical Engineering Science*, 89:223–234, 2013.

[49] Francesca Rapetti and Alain Bossavit. Whitney forms of higher degree. *SIAM Journal on Numerical Analysis*, 47(3):2369–2386, 2009.

[50] J. N. Reddy. *Energy principles and variational methods in applied mechanics*. John Wiley & Sons, 2002.

[51] TD Ringler, John Thuburn, Joseph B Klemp, and William C Skamarock. A unified approach to energy conservation and potential vorticity dynamics for arbitrarily-structured c-grids. *Journal of Computational Physics*, 229(9):3065–3090, 2010.

[52] Markus Schöberl. Differentialgeometrische beschreibung und analyse tor-basierter hamilton'scher systeme. *at-Automatisierungstechnik*, 63(9):672–683, 2015.

[53] Markus Schoberl and Andreas Siuka. Analysis and comparison of port-hamiltonian formulations for field theories-demonstrated by means of the mindlin plate. In *2013 European Control Conference (ECC)*.

[54] Markus Schöberl and Andreas Siuka. Jet bundle formulation of infinite-dimensional port-hamiltonian systems using differential operators. *Automatica*, 50(2):607–613, 2014.

[55] M. Seslija, J. M. A. Scherpen, and A. J. van der Schaft. Explicit simplicial discretization of distributed-parameter port-hamiltonian systems. *Automatica*, 50(2):369 – 377, 2014.

[56] Marko Seslija, Arjan van der Schaft, and Jacquelien M.A. Scherpen. Discrete exterior geometry approach to structure-preserving discretization of distributed-parameter port-hamiltonian systems. *Journal of Geometry and Physics*, 62(6):1509–1531, 2012.

[57] Enzo Tonti. A direct discrete formulation of field laws: The cell method. *CMES- Computer Modeling in Engineering and Sciences*, 2(2):237–258, 2001.

[58] Vincent Trenchant, Hector Ramirez, Yann Le Gorrec, and Paul Kotyczka. Structure preserving spatial discretization of 2D hyperbolic systems using staggered grids finite difference. In *Proc. American Control Conference (accepted)*, 2017.

[59] A. J. van der Schaft. *L2-Gain and Passivity Techniques in Nonlinear Control.* Springer-Verlag, London, 2000.

[60] A. J. van der Schaft and B. M. Maschke. Hamiltonian formulation of distributed-parameter systems with boundary energy flow. *Journal of Geometry and Physics*, 42(1):166–194, 2002.

[61] A. J. Van der Schaft and B. M. Maschke. Discrete conservation laws and port-hamiltonian systems on graphs and complexes. *arXiv:1107.2006v1*, 2011.

[62] A. J. Van der Schaft and B. M. Maschke. Port-hamiltonian systems on graphs. *SIAM Journal on Control and Optimization*, 51(2):906–937, 2013.

[63] Arjan van der Schaft, Dimitri Jeltsema, et al. Port-Hamiltonian systems theory: An introductory overview. *Foundations and Trends® in Systems and Control*, 1(2-3):173–378, 2014.

[64] Ngoc Minh Trang Vu, Laurent Lefèvre, Rémy Nouailletas, and Sylvain Brémond. Symplectic spatial integration schemes for systems of balance equations. *Journal of Process Control*, 51:1–17, 2017.

[65] Trang Vu, Laurent Lefevre, and Bernhard Maschke. Port-hamiltonian formulation for systems of conservation laws: Application to plasma dynamics in tokamak reactors. In *Lagrangian and Hamiltonian Methods for Non Linear Control*, volume 4, pages 108–113, 2012.

[66] H. Whitney. Geometric integration theory. *Princeton UP, Princeton*, 1957.

[67] H. Zwart, Y. Le Gorrec, and B. Maschke. Building systems from simple hyperbolic ones. *Systems & Control Letters*, 2016.

Beachte JCP Sonderheft: Journal of Computational Physics, Volume 257, Part B, Pages 1039-1526 (15 January 2014) Physics-compatible numerical methods